

1 Treatment of non-ideality in the multiphase model 2 SPACCIM- Part I: Model development

3

4 **A. J. Rusumdar^{1,*}, R. Wolke¹, A. Tilgner¹, and H. Herrmann¹**

5 [1]{Leibniz Institute for Tropospheric Research (TROPOS), Leipzig, Germany}

6 [*]{Institute for Micro Process Engineering, Karlsruhe Institute of Technology, Germany}

7 Correspondence to: R. Wolke (wolke@tropos.de)

8

9 **Abstract**

10 Ambient tropospheric deliquesced particles generally comprise a complex mixture of
11 electrolytes, organic compounds, and water. Dynamic modeling of physical and chemical
12 processes in this complex matrix is challenging. Thus, up-to-date multiphase chemistry
13 models generally do not consider non-ideal solution effects. Therefore, the present study was
14 aimed at presenting further development of the SPACCIM (Spectral Aerosol Cloud
15 Chemistry Interaction Model) model through treatment of solution non-ideality, which has not
16 been considered before. The present paper firstly describes the model developments including
17 (i) the implementation of solution non-ideality in aqueous-phase reaction kinetics in the
18 SPACCIM framework, (ii) the advancements in the coupling scheme of microphysics and
19 multiphase chemistry and (iii) the required adjustments of the numerical schemes, especially
20 in the sparse linear solver and the calculation of the Jacobian. Secondly, results of sensitivity
21 investigations are outlined aiming at the evaluation of different activity coefficient modules
22 and the examination of the contributions of different intermolecular forces to the overall
23 activity coefficients. Finally, first results obtained with the new model framework are
24 presented.

25 The parcel model SPACCIM was developed and, so far, applied for the description of
26 aerosol-cloud interactions. To advance SPACCIM also for modeling physical and chemical
27 processes in deliquesced particles, the solution non-ideality have to be taken into account by
28 utilizing activities in reaction terms instead of aqueous concentrations. The main goal of the
29 extended approach was to provide appropriate activity coefficients for solved species.
30 Therefore, an activity coefficient module was incorporated in the kinetic model framework of

1 SPACCIM. Based on an intercomparison of different activity coefficient models and the
2 comparison with experimental data, AIOMFAC approach was implemented and extended by
3 additional interaction parameters from literature for mixed organic-inorganic systems.
4 Moreover, the performance and the capability of the applied activity coefficient module were
5 evaluated by means of water activity measurements, literature data and results of other
6 activity coefficient models. Comprehensive comparison studies showed that the SpactMod
7 (SPACCIM activity coefficient module) is valuable to predict the thermodynamic behavior of
8 complex mixtures of multicomponent atmospheric aerosol particles. First simulations with a
9 detailed chemical mechanism have demonstrated the applicability of SPACCIM-SpactMod.
10 The simulations indicate that, the treatment of solution non-ideality might be needed for
11 modeling multiphase chemistry processes in deliquesced particles. The modeled activity
12 coefficients implicate that chemical reaction fluxes of chemical processes in deliquesced
13 particles can be both decreased and increased depending on the particular species involved in
14 the reactions. For key ions, activity coefficients on the order of 0.1-0.8 and a strong
15 dependency on the charge state as well as the r.h. conditions are modeled implicating a
16 lowered chemical processing of ions in concentrated solutions. In contrast, modeled activity
17 coefficients of organic compounds are in some cases larger than 1 under deliquesced particle
18 conditions and suggest the possibility of an increased chemical processing of organic
19 compounds. Moreover, the model runs have shown noticeable differences in the pH values
20 calculated with and without consideration of solution non-ideality. On average, the predicted
21 pH values of the simulations considering solution non-ideality are -0.27 and -0.44 pH units
22 lower under 90% r.h. and 70% r.h. conditions, respectively. More comprehensive results of
23 detailed SPACCIM-SpactMod studies on the multiphase processing in organic-inorganic
24 mixtures of deliquesced particles are described in a companion paper.

1 **1 Introduction**

2 The troposphere is a complex multiphase and multicomponent environment with
3 simultaneous occurrence of heterogeneous chemical transformations, which potentially can
4 alter the composition of tropospheric aerosols (Ravishankara, 1997). In order to access the
5 impact of physico-chemical and dynamical processes associated with aerosol particles, a
6 variety of multiphase chemistry mechanisms have been developed and coupled with
7 atmospheric models (Binkowski and Roselle, 2003; Fast et al., 2006; Seinfeld and Pandis,
8 2006). During the last decade, some progress was made evaluating the role of chemical
9 aqueous phase processes in deliquesced particles and cloud droplets (see e.g., Hallquist et al.
10 (2009); Tilgner and Herrmann (2010); Ervens et al. (2011); Tilgner et al. (2013); Guo et al.
11 (2014)). Beside the multiphase chemistry developments and findings, the inclusion of reliable
12 thermodynamic modules in multiphase models is required in order to adequately calculate the
13 particle deliquescence, associated water content, chemical reactions and phase transfer
14 processes in multicomponent aerosols at given conditions. Furthermore, these modules are in
15 demand to compute the reactive mass transfer driving forces for dynamic gas-particle
16 partitioning of various semi-volatile species considering complex chemical transformations in
17 aqueous phase.

18 The calculation of gas to particle partitioning of water, semi-volatile inorganic and organic
19 compounds requires the corresponding vapor pressures, which depend on the saturation vapor
20 pressures of pure compounds and the activity coefficients in the liquid mixture. The Köhler
21 theory (Köhler, 1936) gives a relation between the equilibrium saturation ratio S_w of water
22 vapor above an aqueous solution droplet and the droplet equilibrium size:

$$23 \quad S_w = \frac{p_w}{p_w^o} = \frac{RH}{100} = a_w \exp\left(\frac{2v_w \sigma_{w,s}}{RT r_{drop}}\right) \quad (1)$$

24 where p_w is the equilibrium partial pressure of water over the solution droplet, p_w^o is the
25 equilibrium water vapor pressure over a flat surface of pure water, RH (-) is the ambient
26 relative humidity; $\sigma_{w,s}$ ($N m^{-1}$) is the droplet solution surface tension; R ($J mol^{-1} K^{-1}$) is the
27 universal gas constant; T (K) is the temperature; r_{drop} (m) is mean wet radius of droplet; and
28 v_w ($m^3 mol^{-1}$) is the partial molar volume of water. The water activity a_w is given as the
29 product of the mole fraction of water x_w in a solution and the molality based water activity

1 coefficient γ_w , which accounts for the effects of all intermolecular interactions that takes
2 place in the solution. Activity coefficients give an indication of the degree of thermodynamic
3 non-ideality. Such non-ideal conditions can be expected in deliquesced particles, where, e.g.,
4 ionic strengths of about 1-45 mol L⁻¹ (Herrmann, 2003; Herrmann et al., 2015) are present. In
5 a highly concentrated solution, ions and non-water molecules are more close to each other;
6 therefore they influence each other through electrostatic forces or other physical interactions.
7 These intermolecular forces modify the affinity of a substance to transfer from one phase into
8 another phase or to enter into a chemical reaction. Hence a recent review by Herrmann et al.
9 (2015) suggested that for modeling of multiphase chemical processes in a concentrated
10 solution, it is reasonable to consider the non-ideal behavior instead of assuming ideal
11 solutions. Thus, activities have to be used instead of concentrations and the appropriate
12 calculation methods have to be employed in multiphase chemistry models. Consequently, a
13 range of sensitivity studies with models accounting for composition dependent processes need
14 to be carried out to clarify the role of the non-ideal behavior, e.g., for the tropospheric
15 multiphase chemistry in deliquesced particles and, overall, its inclusion or neglect in aerosol
16 chemistry models.

17 In order to simulate gas/particle mass transfer in aerosol models, three main approaches (i.e.,
18 equilibrium, kinetic (or dynamic), and hybrid) have been used in literature (Zhang et al.,
19 2004). The equilibrium approach assumes equilibrium between multiple aerosol phases and
20 the ambient gas concentrations reach equilibrium concentrations at the particle surface
21 instantaneously. The kinetic approach does not rely on the instantaneous equilibrium
22 assumption. In this approach, the gas/particle mass transfer due to the difference between the
23 ambient gas concentration and equilibrium gas concentration is explicitly simulated for each
24 particle class. Usually, hybrid models employ the kinetic approach for coarse particles and the
25 equilibrium approach for fine particles. Thus, an aerosol thermodynamic model is an essential
26 part of all three gas/particle mass transfer approaches.

27 Considerable effort has been devoted to develop a number of thermodynamic models with
28 reliable accuracy and efficiency to simulate aerosol thermodynamic equilibrium. These
29 models treat particle compositions of varying levels of complexity, often associated by the
30 numerical technique chosen and the activity coefficient model applied. They can be divided
31 into two types, i.e., equation-based approach and Gibbs free energy minimization approach.
32 In the equation-based approach (e.g. ISORROPIA II, Fountoukis and Nenes (2007), Nenes et

1 al. (1998); EQSAM3, Metzger and Lelieveld (2007), Metzger et al. (2006); EQUISOLV II,
2 Jacobson (1997), Jacobson et al. (1996); MARS-A, Binkowski and Roselle (2003), Saxena et
3 al. (1986); MESA, Zaveri et al. (2005a)) a set of reactions is assumed to occur in the
4 atmospheric chemical system (including both gas phase and aerosol phase). The equilibrium
5 state is predicted through the solution of the nonlinear equations system. In the Gibbs free
6 energy minimization approach (e.g. AIM, Clegg et al. (1998b, 1998a); GFEMIN, Ansari and
7 Pandis (1999a); ADDEM, Topping et al. (2005a, 2005b); UHAERO, Amundson et al. (2006);
8 Amundson et al. (2007)), the equilibrium state of the aerosol system is predicted through the
9 solution of minimization of the Gibbs free energy of the system. Some of the thermodynamic
10 models mentioned above have been compared and evaluated in several studies (Ansari and
11 Pandis, 1999b; Zhang et al., 2000; Yu et al., 2005; Metzger et al., 2006). The equilibrium
12 approach assumes that particles are in thermodynamic equilibrium with the corresponding gas
13 phase, i.e., the mass transfer between the phases is instantaneous. However, this assumption
14 must not be necessarily valid for every compound and condition, for example in case of
15 coarse particles (e.g., Wexler and Seinfeld (1990)). Therefore, the mass transfer has to be
16 described dynamically by using kinetic or hybrid approaches (e.g., MADM by Pilinis et al.
17 (2000)). Such aerosol modules, that treat dynamically gas-particle partitioning of inorganic
18 and organic gases coupled to thermodynamics modules, are developed for the more general
19 use in 3D models (e.g., MOSAIC by Zaveri et al. (2008), MADRID by Zhang et al. (2004)) or
20 for detailed process descriptions in laboratory (e.g., ADCHAM by Roldin et al. (2014)).

21 As mentioned above, determining appropriate activity coefficients is required in the
22 thermodynamic models. This was achieved by using both mixing rules and potentially more
23 accurate techniques for calculating the activity coefficients. Attempts at realistic estimation of
24 activity coefficients can be traced back to extensive literature for inorganic electrolyte
25 solutions (e.g., Prausnitz et al. (1986); Pitzer (1991); Clegg et al. (1998b, 1998a); Nenes et al.
26 (1998); Metzger et al. (2002); Topping et al. (2005a); Zaveri et al. (2005a); Fountoukis and
27 Nenes (2007)). While the interactions between inorganic compounds are relatively well-
28 known, interactions between organic components as well as organic-electrolyte mixtures
29 comprised in complex multiphase systems have remained elusive for some-time, due to the
30 large number of organic species with highly variable properties available in the gas phase and
31 in ambient particles. Starting with the more conceptual paper of Clegg et al. (2001), several
32 approaches for the treatment of organic-inorganic mixtures in ambient particles were
33 developed and incorporated in thermodynamic models (e.g., Ming and Russell (2002);

1 Topping et al. (2005b); Erdakos et al. (2006); Metzger et al. (2006); Clegg et al. (2008);
2 Zaveri et al. (2008); Zuend et al. (2008); Zuend et al. (2011); Ganbavale et al. (2015)).
3 Raatikainen and Laaksonen (2005) have compared different activity coefficient models, and
4 four models were extended by fitting new parameters for aqueous organic-electrolyte
5 solutions. Most of these revised activity coefficient models are based on an extension of the
6 UNIFAC concept. Erdakos et al. (2006) further developed these extended UNIFAC models.
7 Zuend et al. (2008) fitted the interaction parameters for the organic compounds (alcohols and
8 polyols) and inorganic ions. AIOMFAC is based on the group-contribution model LIFAC
9 (Yan et al., 1999) and yet modified in many respects to better represent relevant species,
10 reference states, and the relative humidity range of the atmosphere. Recently, Zuend et al.
11 (2011), Mohs and Gmehling (2013) and Ganbavale et al. (2015) proposed revised and
12 extended parameterizations for mixtures containing various organic functional groups, water
13 and inorganic ions.

14 Complex multiphase chemistry model dealing with deliquesced particles usually do neglect or
15 roughly estimate the effect of solution non-ideality on the chemical processing (see, e.g.,
16 Tilgner and Herrmann (2010); Bräuer et al. (2013); Mao et al. (2013); Tilgner et al. (2013);
17 Guo et al. (2014)). However, model studies (e.g., Bräuer et al. (2013); Tilgner et al. (2013))
18 implicated that deliquesced particles might be a potentially important medium for multiphase
19 chemistry. Thus, the present study was aimed at the implementation of solution non-ideality
20 in aqueous-phase reaction kinetics into the Spectral Aerosol Cloud Chemistry Interaction
21 Model (SPACCIM, Wolke et al. (2005)). Accordingly, an activity module has to be
22 implemented in SPACCIM to provide appropriate activity coefficients for dissolved species.
23 The parcel model SPACCIM was originally developed for the dynamical description of
24 chemical and microphysical cloud processes. SPACCIM was successfully applied in several
25 process studies using the complex multiphase mechanism CAPRAM (Herrmann et al., 2005;
26 Tilgner and Herrmann, 2010; Bräuer et al., 2013; Tilgner et al., 2013).

27 In this paper, we present an extended model approach for the kinetic description of phase
28 transfer and complex multiphase chemistry considering the non-ideality of solutions by means
29 of activity coefficient models. This paper split into 4 sections. In section 2, we described the
30 implementation of solution non-ideality into the SPACCIM model. In subsequent subsections,
31 the coupling between microphysics and multiphase chemistry models as well as the necessary
32 adjustments of numerical schemes is discussed. In Sect. 2.3, the activity coefficient module is

1 introduced, that is specifically designed to treat multicomponent mixed organic–inorganic
2 aerosol particles. Section 3 presents an evaluation of the currently implemented activity
3 coefficient module in SPACCIM. In order to validate the model performance and the
4 capability, the model results were compared with available measurements and other activity
5 coefficient models such as mod. LIFAC (Kiepe et al., 2006), E-AIM (Clegg et al., 1998b, a),
6 and AIOMFAC (Zuend et al., 2008). Furthermore, Sect. 3 presents sensitivity studies on the
7 importance of the different interactions and first model results obtained with the new model
8 framework.

9

10 **2 Methodology and model development**

11 **2.1 Multiphase model SPACCIM (original code)**

12 In this section, a brief summary is provided for the methods used in SPACCIM original
13 code and the current limitations are outlined. The air parcel model SPACCIM was
14 developed for the description of simultaneously occurring chemical and physical processes in
15 cloud droplets and deliquesced particles. Thus, SPACCIM combines a complex multiphase
16 chemistry model with a detailed cloud microphysics for a size-resolved particle/droplet
17 spectrum in a box model framework (Wolke et al., 2005). Depending on the used
18 microphysical model, external and internal mixing of aerosol can be taken into account. The
19 activation of droplets is explicitly described. Either the movement of the air parcel can follow
20 a predefined trajectory (e.g., simulated by a 3D atmospheric model) or the vertical velocity is
21 calculated based on the parcel updraft compared to prescribed environmental conditions.
22 Entrainment and detrainment processes are considered in a parameterized form. The model
23 allows a detailed description of the processing of gases and particles shortly before cloud
24 formation, during the cloud life time and shortly after cloud evaporation (Sehili et al., 2005).
25 The droplet activation depending on the particle size and composition is explicitly described
26 (see Sehili et al. (2005) and Wolke et al. (2005)).

27 All microphysical parameters needed by the multiphase chemistry are taken over from the
28 microphysical model. For this purpose, a robust and efficient coupling scheme between
29 microphysical and multiphase chemical models is implemented. The coupling scheme is
30 adjusted to the applied time integration method and provides time-interpolated values of the
31 microphysical parameters (temperature, water vapor, liquid water content) and time-averaged

1 mass fluxes between different droplet classes caused by microphysical processes (e.g., by
2 aggregation, break up, condensation). Changes of the chemical aerosol composition by gas
3 scavenging and chemical reactions feed back on the microphysical processes (e.g., water
4 condensation growth rates via changes in the Raoult term). Consequently, related processes
5 such as co-condensation (see Topping et al. (2013) for details) are considered in the model.

6 The multiphase chemistry is performed for ideal solutions assuming well-mixed droplets.
7 Activity coefficients and the diffusion inside of the droplets are not considered. Dissociations
8 are described dynamically as forward and backward reactions. The applied multiphase
9 chemical mechanism (including phase transfer data and kinetic reaction constants) is provided
10 as an input file. Therefore, a high flexibility concerning changes in the chemical mechanism
11 or the replacement of the entire reaction system is guaranteed. For further details, the reader
12 is referred to the original publication by (Wolke et al., 2005). The performance of the model
13 was shown for both simple chemical mechanisms considering inorganic chemistry only and
14 for very complex mechanisms of the CAPRAM family, which contain a detailed description
15 of the inorganic and organic chemistry (Herrmann et al., 2005; Tilgner and Herrmann, 2010;
16 Bräuer et al., 2013; Tilgner et al., 2013).

17 In the published version of SPACCIM (Wolke et al., 2005), the influence of solution non-
18 ideality on multiphase processing was not considered. In fact, the assumption of an ideal
19 solution is not valid particularly for deliquescent particles, where highly concentrated
20 solutions are typical present. Accordingly, the chemical reaction terms in the aqueous phase
21 chemistry have to be modified by using the activities and therefore an activity coefficient
22 module has to be added. Furthermore, the feedback approach is enhanced by using the
23 calculated water activity for the Raoult term and by the consideration of surface tension
24 effects. The changes in the model code are given in the following subsection.

25 **2.2 Further development of SPACCIM**

26 **2.2.1 Mass balance equations**

27 For the consideration of solution non-ideality effects in SPACCIM, it is required that rate
28 expressions have to be written in terms of species activities, rather than mole fractions or
29 concentrations. The activity a_i of species i can be expressed by $a_i = \gamma_i \cdot m_i = \gamma_i \cdot c_i / L$ where
30 γ_i denotes the molality based activity coefficient, m_i the molality and c_i the mass

1 concentration of an aqueous phase species i . The liquid water content L is given as the water
 2 mass in the corresponding box volume. In the proposed approach, the non-ideal behavior is
 3 taken into account by means of activity coefficients. It should be emphasized that the activity
 4 coefficient γ_i depends usually on the concentrations of all species dissolved in the solution.

5 In Eqs. (1) and (2), the mass balance equations of the modified version of SPACCIM
 6 extended by the treatment of solution non-ideality are presented. In particular, the aqueous
 7 concentrations in the original mass balance equations of the SPACCIM (see Eqs. (1) and (2)
 8 in Wolke et al. (2005)) are replaced by corresponding activities.

9 The description of both microphysical and multiphase chemical processes is performed for a
 10 size-resolved particle/cloud droplet spectrum, which is subdivided into several classes
 11 $k = 1, \dots, M$. In each particle/droplet class, N_A aqueous phase species are treated, which are
 12 not necessarily identical to the number of gas phase species N_G . In the parcel model
 13 SPACCIM, the prognostic equations for the mass concentrations of a gas phase chemical
 14 species $c_{i^*}^G$ and an aqueous phase chemical species c_i^k in the k^{th} class have to take into
 15 account the chemical productions and degradations, phase transfers, mass transport between
 16 different classes caused by microphysical processes, and ent-/detrainment. These processes
 17 can be described by the following mass balance equations:

$$18 \quad \frac{d(c_{i^*}^G)}{dt} = \underbrace{R_{i^*}^G(t, c_1^G, \dots, c_{N_G}^G)}_{\text{gas phase chemistry}} - \underbrace{\kappa_i \sum_k L_k k_t^{ki} \left[c_{i^*}^G - \frac{a_i^k}{H_i} \right]}_{\text{phase transfer}} + \underbrace{\mu [c_{i^*}^G - c^{G_{ent}}]}_{\text{entrainment / outflow}}, \quad (2)$$

$$19 \quad \frac{d(c_i^k)}{dt} = \underbrace{L_k R_i^A(t, a_1^k, \dots, a_{N_A}^k)}_{\text{aqueous phase chemistry}} + \underbrace{\kappa_i L_k k_t^{ki} \left[c_{i^*}^G - \frac{a_i^k}{H_i} \right]}_{\text{phase transfer}} + \underbrace{F(c_i^1, \dots, c_i^M)}_{\text{mass transfer by microphysics}} + \underbrace{\mu [c_i^k - c_i^{k_{ent}}]}_{\text{entrainment / outflow}}, \quad (3)$$

20 with $i^* = 1, \dots, N_G$; $i = 1, \dots, N_A$; $k = 1, \dots, M$.

21 In the above formulation, L_k denotes the liquid water content of the k^{th} droplet class inside
 22 the box volume. The values $a_i^k, k = 1, \dots, M$, represent the activities of species i in the k^{th}
 23 liquid water fraction. The vector c^G stands for the concentrations of the gas phase species
 24 and k_t^{ki} is the mass transfer coefficient. The chemical reaction terms of the corresponding
 25 species are denoted by $R_{i^*}^G$ and R_i^A . The second term on the right-hand side of the

1 aforementioned equations describe the change of mass concentration of the soluble species
 2 due to phase transfer between the gas phase and particle/cloud droplet classes. Hence, this
 3 term will be referred to as the Henry term in the following. The value H_i denotes here the
 4 dimensionless Henry's law coefficient for species i . The prefactor κ_i of the Henry term is a
 5 solubility index and defined to be equal to 1 as well as 0 for soluble and insoluble species,
 6 respectively (see Wolke et al. (2005)). The term $F(c_i^1, \dots, c_i^M)$ in Eq. (3) stands for the mass
 7 transfer between different droplet classes by microphysical exchange processes (e.g. by
 8 aggregation, break up, condensation). The time-dependent natural and anthropogenic
 9 emissions as well as dry and wet deposition are parameterized in the last terms of the right
 10 hand sides using a time dependent entrainment/detrainment rate μ . One should note that,
 11 above-mentioned mass balance equations are not only limited to "non-ideal" approach.
 12 Whenever, the activity coefficients are defined as unity then this numerical model formulation
 13 will reduce to the original version of SPACCIM.

14 2.2.2 Reaction kinetics

15 The first terms $R_{i^*}^G$ and R_i^A in the right hand sides of the mass balance Eqs. (2) and (3)
 16 comprise the chemical transformations (production and degradation fluxes). However, the
 17 reaction term included in Eq. (2) is only a function of concentrations of gas phase species.
 18 Since, the gas phase mixture is assumed to be behaving as an ideal gas phase mixture, the
 19 non-ideality is not considered in this term.

20 Suppose, for an irreversible reaction $A + B \rightarrow C + D$ in the aqueous phase, the reaction rate
 21 r_A can be written while considering the solution non-ideality as follows:

$$22 \quad r_A = -k_A \cdot [a_A] \cdot [a_B] = -k_A \cdot \gamma_A [A] \cdot \gamma_B [B], \quad (4)$$

23 Here, the activities of A, B, C, and D are used instead of the concentrations. The activity of A
 24 (a_A) is proportional to its molar concentration (either molality based or mole fraction based)
 25 $[A]$, where the proportional constant is the activity coefficient γ_A of that particular species.
 26 The treatment of solution non-ideality was also considered for equilibrium reaction types,
 27 which should be explained with the generic example shown as:



29 The relative quantities (i.e. thermodynamic activities) of reactants and products in an

1 equilibrium reaction are determined from the equilibrium relation,

$$2 \quad \sum_i \{a_i\}^{\lambda_i v_i} = \frac{\{A\}^{v_A} \cdot \{B\}^{v_B}}{\{C\}^{v_C} \cdot \{D\}^{v_D}} = \frac{(\gamma_A^{v_A} \cdot [A]^{v_A}) \cdot (\gamma_B^{v_B} \cdot [B]^{v_B})}{(\gamma_C^{v_C} \cdot [C]^{v_C}) \cdot (\gamma_D^{v_D} \cdot [D]^{v_D})} = K_{eq}, \quad (6)$$

3 where K_{eq} called as equilibrium coefficient, $\{a_i\}$ is the thermodynamic activity of species i ,
4 $\{A\}$, etc., are individual thermodynamic activities, $\lambda_i = +1$ for products, and $\lambda_i = -1$ for
5 reactants. As mentioned earlier, activity of a species A is its molality m_A multiplied by its
6 activity coefficient γ_A . A solute activity coefficient represents the deviation from ideal
7 behavior of the solute in solution. Hence, the concentration dependent activity coefficients are
8 estimated for all soluble species. Note, that the activity coefficients for neutral inorganic
9 species (such as $O_{2(aq)}$) are defined as unity. At the same time, the activity coefficients of
10 radicals are also defined as unity, since their reactivity is quite fast and lifetime is rather
11 small. The consideration of activities in the SPACCIM framework for different types of
12 species is summarized in Table 1.

13 2.2.3 Phase transfer processes

14 The dynamical description of phase transfer processes between the gas and liquid phases in
15 SPACCIM is specified according to the Schwartz approach (Schwartz, 1986). During
16 dissolution, the saturation vapor pressure of gas A can be determined from the equilibrium
17 relationship $A_{(g)} \rightleftharpoons A_{(aq)}$. Thus, in terms of an arbitrary gas i the Henry's law is defined as:

$$18 \quad p_{i,k}^s = \frac{m_i^k}{K_i^H}, \quad (7)$$

19 where $p_{i,k}^s$ is the saturation vapor pressure (atm) of gas phase species i over a particle in size
20 bin k , m_i^k (mol kg^{-1}) is the molality of dissolved gas phase species i in particle class k , and
21 K_i^H ($\text{mol kg}^{-1} \text{atm}^{-1}$) is the corresponding Henry constant. It has to be noted here that the
22 Henry's law constants of an aqueous solution depend on the composition of the aqueous
23 solution, e.g., on the electrolyte identity of the solution (ionic strength, etc.). Non-ideal
24 electrolyte solutions are able to both suppress the uptake ("salting-out") and enhance the
25 uptake ("salting-in") of soluble gases compared to value for pure water uptake (Herrmann et
26 al., 2015). These salting effects can be quantitatively described by the Setschenow equation

1 (Sander, 2015). However, as reported in the review of Sander (2015), there are unfortunately
 2 only limited data available. Therefore, salt effects are only considered in the SPACCIM
 3 model due to the consideration of the activity coefficients in the uptake calculation. The
 4 model results should be therefore treated with caution particularly at higher ionic strengths of
 5 the solution due to the lower range of functionality of Henry's law coefficients compared to
 6 the applicability range of present activity coefficient models.

7 The above-mentioned saturation vapor pressure is related to the saturation vapor mole
 8 concentration $c_{i,k}^s$ (mol m⁻³) by

$$9 \quad p_{i,k}^s = c_{i,k}^s RT, \quad (8)$$

10 where R denotes the universal gas constant in (atm m³ mol⁻¹ K⁻¹) and T (K) the temperature.
 11 Then, Eq. (7) can be expressed in terms of concentrations rather than molalities and partial
 12 pressures as:

$$13 \quad c_{i,k}^s = \frac{p_{i,k}^s}{RT} = \frac{m_i^k}{K_i^H RT} = \frac{m_i^k}{H_i}. \quad (9)$$

14 Here $H_i = K_i^H RT$ stands for the dimensionless Henry constant. Considering the solution non-
 15 ideality in the aqueous phase, the molalities m_i^k are replaced by the activities $a_i^k = \gamma_i^k m_i^k$.
 16 Considering M classes of particles associated, we state the appropriate expression for gas-
 17 phase loss while neglecting the Kelvin effect (following Jacobson (1997)):

$$18 \quad \frac{dc_i^G}{dt} = -\sum_k k_t^{ki} L_k \left(c_i^G - \frac{a_i^k}{H_i} \right). \quad (10)$$

19 Eq. (10) pertains to the case of a single gas phase species equilibrating between the gas and
 20 aqueous aerosol phases, with the mass transfer coefficient k_t^{ki} defined by

$$21 \quad k_t^{ki} = \left(\frac{r_k^2}{3D_i^G} + \frac{4r_k}{3v_i \alpha_i} \right), \quad (11)$$

22 which depends on the droplet size r_k , the gas diffusion coefficient D_i^G , the molecular speed v_i
 23 and the mass accommodation coefficient α_i of the i^{th} species. These quantities play a
 24 decisive role in determining the rate of uptake of gaseous species by, and evaporation from

1 aerosol particles, respectively, governing the timescale for a droplet to attain an equilibrium
2 (Schwartz, 1986).

3 2.2.4 Coupling scheme

4 The coupling between microphysics and multiphase chemistry models in SPACCIM follows
5 the so-called “operator splitting” technique. As described in Sehili et al. (2005), the coupling
6 scheme provides time-interpolated values of the meteorological variables (temperature, water
7 vapor, liquid water content) and generates the time-averaged mass fluxes F over the coupling
8 time interval. The changes in the chemical aerosol composition by gas scavenging and the
9 chemical reactions have a continuous feedback on the microphysical processes (e.g. water
10 condensation growth rates via changes in surface tension and the Raoult term/water activity).

11 For the “non-ideal” approach in SPACCIM, the coupling scheme is modified, since activity
12 coefficients have to be considered in both models. At the same time, the activity coefficients
13 are repeatedly required to compute the chemical transformations and the phase transfer terms
14 (see Sect. 2.2.2 and 2.2.3). Furthermore, the modified activity coefficients as well as the
15 parameterized surface tension are delivered back to the microphysical model. Fig. 1 illustrates
16 this coupling strategy between microphysical and multiphase chemistry model as well as their
17 interexchange while considering non-ideal solutions and surface tension effects (see Sect.
18 2.2.6). The coupling strategy enables a continuous feedback of the multiphase chemistry on
19 the microphysical processes such as water condensational growth. The two models run
20 separately and exchange information at every coupling time step (see Fig. 2). Moreover, both
21 widely separated operating models use its individual time-step control. This is necessary in
22 order to ensure a high flexibility regarding the usage of models with different complexities
23 and numerical efficiency. The coupling between both models and the activity coefficient
24 module utilize well-defined interfaces for the intercommunication of codes while considering
25 the aqueous phase chemistry in non-ideal solutions. Furthermore, the interpolation and
26 averaging of the required meteorological variables and parameters are arranged and
27 implemented in the same way as described in Wolke et al. (2005).

28 2.2.5 Feedback of non-ideal aqueous phase chemistry on microphysics

29 Microphysical processes described in SPACCIM include equilibrium growth of aerosol
30 particles and condensational growth of the droplets (Simmel and Wurzler, 2006). The Köhler
31 equation (see e.g., Köhler (1936); Pruppacher and Klett (1997)) gives the saturation ratio of

1 water vapor at particle/air interface, which depends on the chemical composition, the droplet
 2 diameter and the surface tension of the particle. In SPACCIM, the non-linear relationship
 3 Eq. (1) is used to determine the equilibration of water between the liquid and surrounding
 4 vapor phase for non-activated particles. The water saturation pressure in Eq. (1) is affected by
 5 the curvature of the particle (also known as Kelvin effect) and the water activity, which is
 6 determined by the solutes (Raoult effect). Previously, Wolke et al. (2005) calculated the
 7 Raoult term in the condensation rate using osmotic coefficient, according to Pruppacher and
 8 Klett (1997). While, the intention was to allow the feedback of chemical particle composition
 9 onto microphysics, the Raoult term was replaced by the sum of molar ratios of all soluble
 10 species included in the multiphase system:

$$11 \quad Raoult_{chem}^k = \frac{\sum_i^{N_A} mol_{sol_i}^k}{mol_w^k}. \quad (12)$$

12 Here, the quantities $mol_{sol_i}^k$ of soluble material are obtained from the multiphase chemistry.
 13 The molar water fraction mol_w^k varies and is taken directly from the microphysics. The Raoult
 14 term in Eq. (12) depends on all soluble species. In the non-ideal approach of SPACCIM, the
 15 water activity a_w^k estimated from activity coefficient module (see Sect. (2.3)), is used directly
 16 for the Raoult term in microphysics. On the other hand, the description of change in droplet
 17 curvature (Kelvin effect) is treated with surface tension approaches (see Subject. 2.2.6).

18 Both effects are influenced by the particle composition, which is continuously changed by
 19 phase transfer and multiphase processes. However, the mass concentrations of all species are
 20 kept fixed for the microphysics over a coupling time step (see Fig. 1). But the molalities and,
 21 therefore, the Kelvin and Raoult terms are changed caused by the adjustment of the liquid
 22 water content. Eq. (1) has to be fulfilled simultaneously for all non-activated particle classes.
 23 The droplet activation is described explicitly and takes place for all particles, which grow
 24 over the critical radius. The condensation and evaporation of the activated droplet classes are
 25 described dynamically. The predicted saturation vapor pressure is used as input into the
 26 droplet growth equation. The coupled system for all classes has to be solved simultaneously,
 27 whereas the total amount of water (liquid or gaseous) is prescribed. This leads to a nonlinear
 28 system, which has to be solved iteratively at each microphysical time step. A more detailed
 29 description of the iterative procedure is given in Simmel and Wurzler (2006). A new solution
 30 of the system is obtained, and defines the equilibrium saturation ratio and the corresponding

1 particle/droplet diameters. This implies changes in the corresponding liquid water contents
2 and, hence, in the molalities. Consequently, the water activity and the surface tension have to
3 be recalculated at each microphysical time step. A description of the equilibration algorithm is
4 presented schematically in Fig. 2. Based on this, SPACCIM allows an ongoing feedback of
5 the chemical particle composition onto microphysics. Conversely, the microphysical model
6 provides all microphysical variables for integrating the multiphase chemical system, such as
7 liquid water content, T and the mass fluxes F at the coupling time step (see Fig. 1).

8 2.2.6 Surface tension

9 Surface-active substances present at the interface and organic compounds dissolved in the
10 solution can significantly influence the surface tension and thus can affect cloud droplet
11 activation and hygroscopic growth (Shulman et al., 1996; Facchini et al., 2000; Tuckermann
12 and Cammenga, 2004; Topping et al., 2007; Prisle et al., 2012). A reduction of surface
13 tension in atmospheric cloud and fog water samples was highlighted in several studies (e.g.,
14 Facchini et al. (1999); Facchini et al. (2000); Mircea et al. (2002); Nenes et al. (2002)).
15 Furthermore, Henning et al. (2005) and Svenningsson et al. (2006) measured a surface tension
16 lowering for organic mixtures in laboratory studies. On the other hand, Sorjamaa et al. (2004)
17 and Sorjamaa and Laaksonen (2006) pointed out that surface-active substances can enrich at
18 the particle/droplet surface.

19 A first specific relationship between water-soluble organic aerosol concentration and surface
20 tension has been derived by fitting the equation of Szyszkowski-Langmuir to Po Valley fog
21 data (Facchini et al., 1999). Model approaches that can estimate the surface tension of
22 inorganic, organic systems and mixed inorganic/organic systems were proposed by Topping
23 et al. (2007). Recently, sophisticated parameterizations were developed for modeling the
24 combined effects of both bulk-surface partitioning and surface tension on cloud droplet
25 activation of organic aerosols (Topping (2010); Prisle et al. (2011); Raatikainen and
26 Laaksonen (2011)). However, Prisle et al. (2012) suggested neglecting the surfactant effects
27 instead of employing the numerical parameterizations calculating the reduction of surface
28 tension.

29 Since the present paper is aimed at the treatment of solution non-ideality in a multiphase
30 chemistry model framework, the model development considered the influence of surface
31 tension on droplet activation, as a first step, with more simplified parameterizations of

1 Facchini et al. (1999) and Ervens et al. (2004) only. The implementation of more advanced
2 approaches in SPACCIM will be subject of future development efforts.

3 In the present work, the following relationship proposed by Facchini et al. (1999) was
4 implemented in the SPACCIM framework:

$$5 \quad \sigma_{w,s}^k = \sigma_w^k - 0.01877 \cdot T \cdot \ln(1 + 628.14 \cdot [C^k]), \quad (13)$$

6 where T is the temperature in K and $[C^k]$ represents the concentration of WSOC (Water
7 Soluble Organic Carbon, mol C L⁻¹) in particle class k . In addition, a combined approach for
8 accounting for a simultaneous change in $\sigma_{w,s}^k$ and the mean molar mass of solute M_{sol} derived
9 by Ervens et al. (2004) was also implemented in the present work:

$$10 \quad \sigma_{w,s}^k = \sigma_w^k - 0.01877 \cdot T \cdot \ln(1 + 628.14 n_c c_{sol}^k), \quad (14)$$

11 where c_{sol}^k is the solute concentration in (mol L⁻¹) and n_{cb} represents the number of carbon
12 atoms defined by

$$13 \quad n_{cb} = \frac{M_{sol}}{2.2 M_c}, \quad (15)$$

14 with $M_c = 12 \text{ g mol}^{-1}$.

15 2.2.7 Adjustment of numerical schemes

16 In order to treat aqueous phase chemistry considering newly solution non-ideality effects, the
17 numerical schemes used in Wolke et al. (2005) are required to adjust, mainly, (i) the time
18 integration scheme, (ii) the computation of Jacobian matrix and (iii) the sparse linear solver.
19 The system of mass balance equations (Eqs. (2) and (3)) is integrated in an implicit and
20 coupled manner by higher order backward differential formula (BDF) schemes (e.g., Hairer et
21 al. (1993)). In any implicit multistep method, the main computational task is the solution of a
22 non-linear equation of the form:

$$23 \quad \mathbf{F}(\mathbf{c}^{n+1}) = \mathbf{c}^{n+1} - \mathbf{X}^n - \beta \Delta t_n \mathbf{f}(t_{n+1}, \mathbf{c}^{n+1}) = 0, \quad (16)$$

24 where $\mathbf{f}(t_{n+1}, \mathbf{c}^{n+1})$ stands for the right hand side of Eqs. (2) and (3), $\beta > 0$ is a parameter of
25 the integration method and \mathbf{X}^n is a linear combination of previous values. If equation (16) is

1 solved by a Newton-like method, the main burden is the approximate solution of linear
2 systems of the form:

$$3 \quad (\mathbf{I} - \beta \Delta t \mathbf{J}) \Delta \mathbf{c} = \mathbf{b} \quad (17)$$

4 where I denotes the identity matrix and Δt represents the time step size. The matrix \mathbf{J} stands
5 for an approximation of the Jacobian $\partial \mathbf{f}(t, \mathbf{c}) / \partial \mathbf{c}$ of the right hand side of the ordinary
6 differential equation (ODE) system. The vector \mathbf{b} is given as:

$$7 \quad \mathbf{b} = \mathbf{c}^n - \mathbf{X}^n - \beta \Delta t_n \mathbf{f}(t_n, \mathbf{c}^n) \quad (18).$$

8 Usually, the dimension of the linear system Eq. (17) is rather high. Large systems can be
9 solved with reasonable effort by iterative or direct sparse solvers, which utilize the special
10 structure of the system (sparsity, block structure, different types of coupling). Such efficient
11 solvers are already developed and applied in the former version of SPACCIM for the “ideal”
12 approach (see Wolke and Knoth (2002); Wolke et al. (2005) for further details).

13 In this case, the Jacobian structure of the right-hand side of the multiphase system (Eq. (2)
14 and Eq. (3)) for two droplet classes is shown in Fig. 3. As can be seen, the dots are usually
15 non-zero entries means that the species in the row depends on the species in the column. The
16 diagonal elements of the Jacobian describe the dependence from the species itself. These
17 entries can be caused by chemical reactions and phase transfer, but also by the terms from
18 microphysical fluxes and entrainment.

19 The block structure shown in Fig. 3 can be explained as follows: the blocks in the diagonal
20 correspond to the Jacobian of the gas phase and aqueous phase reaction terms, respectively.
21 The upper left block (light blue) represents the gas phase. The other two diagonal blocks
22 (blue) are related to the aqueous phase chemistry attained to have the same sparse structure.
23 The left and upper boundary blocks (green) represent the phase interchange between gas
24 phase species and corresponding aqueous phase species in each class, according to (Schwartz,
25 1986). The orange diagonal matrices include the coupling terms resulting from the mass
26 transfer between liquid species and the corresponding species in the other classes. These
27 sparse block matrices are generated explicitly and stored in sparse form. The linear system
28 (see Eq. (18)) is solved by a sparse LU decomposition with diagonal pivoting. An optimal
29 order of the pivot elements to avoid fill-in is determined by an adjusted Meis–Markowitz
30 strategy (Wolke and Knoth, 2002). In fact, only an appropriate approximation of the Jacobian

1 is required to ensure the convergence of the Newton-like method for the corrector iteration
 2 (Eq. (17)). Therefore, the sparse factorization is stored and has to be performed only when the
 3 Jacobian J is recomputed.

4 The adjusted numerical scheme works robust and very efficient for the “ideal” case. But these
 5 effective approaches can only be used in the ”non-ideal” case, if the special sparse and block
 6 structure can be largely preserved. The calculation of the Jacobian has to be performed by
 7 applying the “chain rule” for the aqueous phase reaction and mass transfer terms in the model
 8 equations Eq. (2) and Eq. (3). These terms depend on the activities instead of the molalities in
 9 difference to the ideal case. While the “outer” derivatives are unchanged, the “inner”
 10 derivatives have to be modified. In case that c^k is the vector of all concentrations and L^k the
 11 liquid water content in the k^{th} droplet class, the gradient with respect to vector \mathbf{c}^k is denoted
 12 as

$$13 \quad \nabla_{\mathbf{c}^k} = \left(\frac{\partial}{\partial \mathbf{c}_1^k}, \dots, \frac{\partial}{\partial \mathbf{c}_{N_A}^k} \right). \quad (19)$$

14 In the ideal approach the molalities depend only on the corresponding species itself. Then the
 15 gradient of the molalities is given as follows:

$$16 \quad \nabla_{\mathbf{c}^k} m_j^k(c_j^k) = \frac{1}{L^k} (0, \dots, 0, 1, 0, \dots, 0). \quad (20)$$

17 In the above formulation, the gradient has only one entry in the j^{th} position, which conserves
 18 the structure of the “outer” Jacobian. Contrary, while applying the chain rule, the gradient for
 19 non-ideal solutions would be:

$$20 \quad \nabla_{\mathbf{c}^k} a_j^k(\mathbf{c}^k) = \frac{c_j^k}{L_k} \cdot (\nabla_{\mathbf{c}^k} \gamma_j^k(\mathbf{c}^k)) + \frac{1}{L_k} \cdot (0, \dots, 0, \gamma_j^k, 0, \dots, 0) \quad (21)$$

21 where the gradient $\nabla_{\mathbf{c}^k} (\gamma_j^k(\mathbf{c}^k))$ of activity coefficients depends usually on all concentrations
 22 of the vector \mathbf{c}^k considered in the activity calculations.

23 The first term in Eq. (21) is a vector with entries in several positions depending on the activity
 24 coefficient module. This leads to “fill-in” in the corresponding lines of the Jacobian from
 25 aqueous phase chemistry (blue blocks) and the phase transfer terms (green blocks).
 26 Consequently, the efficient direct sparse solvers are used in SPACCIM for the linear system

1 cannot be utilized. However, since only a “good” approximation for the Jacobian is needed,
2 the first term shown in Eq. (21) is omitted assuming that the dependency of the activity
3 coefficients from the concentrations can be neglected over the time step. The second term
4 involves the activity coefficient γ_j^k that yields from the derivative of the activity with respect
5 to molality of that particular species m_j . Although, the derivative of activity coefficients is
6 omitted, the same data structures are obtained as in ideal case. The second term on the right
7 hand side of Eq. (21) has the same structure as on the right hand side of Eq. (20). Only the
8 non-zero entry in the j^{th} position changes from 1 to γ_j^k . This leads to modifications of the
9 non-zero entries in the Jacobians of the chemistry (blue blocks) and the phase transfer (green
10 blocks) terms. However, the sparse structure of the systems is conserved effectively.

11 **2.3 SPACCIM’s activity coefficient module**

12 A main task in the extended approach (Fig. 2) is to provide appropriate activity coefficients
13 for the solved species. Therefore, several suitable activity models have been tested and
14 compared regarding their suitable applicability in order to achieve the above-mentioned
15 objective. (see Subsect. 3.1). Overall, AIOMFAC seems to be most qualified for the aimed
16 applications. Therefore, the implementation of the related module SpactMod was performed
17 by using the theoretical framework and the available parameters of Zuend et al. (2008). The
18 AIOMFAC was originally developed for systems composed of organic compounds with $-\text{CH}_n$
19 ($n = 0,1,2,3$) and $-\text{OH}$ as functional groups. On the other hand, several authors (e.g., Gilardoni
20 et al. (2009); Liu et al. (2009); Russell et al. (2009); Takahama et al. (2011)) reported that
21 other individual organic compounds and compound classes have also a strong impact on
22 multiphase chemical processing on ambient aerosols for instance, aldehydes, ketones,
23 carboxylic acids, and multifunctional organic compounds. Moreover, the aforementioned
24 organic compound classes are almost omnipresent in tropospheric aerosol particles and,
25 therefore, explicitly treated in complex multiphase chemistry mechanism such as CAPRAM
26 (see e.g., Herrmann et al. (2005); Tilgner et al. (2013)). Hence, the prediction of the activity
27 coefficients for complex multi-component aerosols, composed of various organic functional
28 groups and electrolytes dissolved in water is the primary purpose of SpactMod. In order to
29 treat various aerosol constituents, additional parameters were included from the mod. LIFAC
30 approach of Kiepe et al. (2006), which can be rewritten in the AIOMFAC formalism (see
31 Appendix A1) and incorporated without new parameter fitting. A compilation of the

1 SpactMod parameters is given in Tables A1-A6. The differences to AIOMFAC are
2 highlighted.

3 2.3.1 Model treatment of solution non-ideality

4 The development of thermodynamic models for mixed-solvent electrolyte systems was an
5 active area of research during the last three decades. In general, these models contain several
6 contributions to describe the system non-ideality, that define the excess Gibbs energy

7 $G^{ex}(p, T, n_j)$:

$$8 \quad G^{ex}(p, T, n_j) = G_{LR}^{ex} + G_{MR}^{ex} + G_{SR}^{ex}, \quad (22)$$

9 where G_{LR}^{ex} represents the long-range (LR) electrostatic interactions, G_{SR}^{ex} is the short-range
10 (SR) contribution resulting from dipole ↔ dipole and dipole ↔ induced dipole interactions,
11 and an additional term (middle-range, MR) G_{MR}^{ex} , which accounts for ionic interactions (e.g.,
12 ion ↔ ion, ion ↔ dipole, ion ↔ induced dipole interactions), p is the total pressure, T the
13 absolute temperature, and $n_j (j = 1, \dots, N)$ the number of moles of component j in a system.

14 Accordingly, the corresponding activity coefficient γ_j^k of a species j with amount of moles n_j
15 in the mixture are derived from expressions for the different parts of G^{ex} using the relation:

$$16 \quad \ln \gamma_j = \left(\frac{\partial G^{ex}/RT}{\partial n_j} \right)_{p, T, n_{j \neq j}}, \quad (23)$$

17 where R is the universal gas constant. Correspondingly, the activity coefficients are calculated
18 from the aforementioned three different contributions:

$$19 \quad \ln \gamma_j = \ln \gamma_j^{LR} + \ln \gamma_j^{MR} + \ln \gamma_j^{SR}. \quad (24)$$

20 2.3.2 The long-range contribution

21 The LR interactions described as they are in original AIOMFAC, based on the Debye-Hückel
22 theory (Debye and Hückel, 1923). In contrast to other works Li et al. (1994); Yan et al.
23 (1999); Chang and Pankow (2006), AIOMFAC uses the water properties for all solvent
24 components for density and dielectric constant of the solvent mixture, instead of using mixing
25 rules. With this assumption, the corresponding LR activity coefficient expressions for the
26 solvents and ions are defined according to Zuend et al. (2008) as

$$\ln \gamma_s^{LR(x)} = \frac{2AM_s}{b^3} \left(1 + b\sqrt{I} - \frac{1}{1+b\sqrt{I}} - 2\ln(1+b\sqrt{I}) \right), \quad (25)$$

$$\ln \gamma_i^{LR(x),\infty} = \frac{-z_i^2 A \sqrt{I}}{1+b\sqrt{I}}. \quad (26)$$

Eq. (26) gives the activity coefficient of ion i in the mole fraction basis (x) with the reference state of infinite dilution in water, indicated by super script ∞ . M_s represents the molar mass of solvent s and z_i is the number of elementary charges of ion i . The ionic strength I (mol kg^{-1}) is given as

$$I = \frac{1}{2} \sum_i m_i z_i^2 \quad (27)$$

with the Debye-Hückel parameters:

$$A = 1.327757 \cdot 10^5 \cdot \frac{\sqrt{\rho_w}}{(\epsilon_w T)^{3/2}}, \quad (28)$$

$$b = 6.359696 \cdot \sqrt{\frac{\rho_w}{(\epsilon_w T)}}. \quad (29)$$

The Debye-Hückel parameters A ($\text{kg}^{1/2} \text{mol}^{-1/2}$) and b ($\text{kg}^{1/2} \text{mol}^{-1/2}$) depend on temperature T (K), density ρ_w (kg/m^3) and static permittivity ϵ_w ($\text{C}^2 \text{J}^{-1} \text{m}^{-1}$) of water, calculated based on a distance of closest approach between ions (see Demaret and Gueron (1993); Antypov and Holm (2007)).

Moreover, this simplification to a water-property based expression for LR activity coefficients are favorable, due to the uncertainties to estimate unknown dielectric constants of certain organic compounds and maintaining the thermodynamic consistency regarding the selection of reference states (see Raatikainen and Laaksonen (2005); Zuend et al. (2008)). In a real mixture, solvents have densities and dielectric properties different from those of pure water. For this reason, these simplifications of the LR part were made in other mixed solvent models in chemical engineering and technical chemistry applications (see Iliuta et al. (2000)). The uncertainties occurred due to the adopted assumptions to derive the LR and SR activity coefficients with respect to approximations of parameters, were described in the semi-empirical SR part as in the original AIOMFAC (Zuend et al., 2008).

1 2.3.3 The Middle-range contribution

2 The G_{MR}^{ex} term is the contribution of the indirect effects of the ionic interactions such as ion
 3 \leftrightarrow dipole interactions and ion \leftrightarrow induced dipole interactions to the excess Gibbs energy. For
 4 any mixture containing n_k , ($k=1, \dots, s$) moles of solvent k (main groups of organics and
 5 water) and n_i moles of ion i , G_{MR}^{ex} can be expressed as described by Zuend et al. (2008):

$$\begin{aligned}
 \frac{G_{MR}^{ex}}{RT} = & \frac{1}{\sum_k n_k M_k} \sum_k \sum_i B_{k,i}(I) n_k n_i \\
 & + \frac{1}{\sum_k n_k M_k} \sum_c \sum_a B_{c,a}(I) n_c n_a \\
 6 \quad & + \frac{1}{\sum_k n_k M_k} \sum_c \sum_a C_{c,a}(I) n_c n_a \sum_i \frac{n_i |z_i|}{\sum_k n_k M_k} \quad (30) \\
 & + \frac{1}{\sum_k n_k M_k} \sum_c \sum_{c' \geq c} R_{c,c'}(I) n_c n_{c'} \\
 & + \frac{1}{\left(\sum_k n_k M_k\right)^2} \sum_c \sum_{c' \geq c} \sum_a Q_{c,c',a}(I) n_c n_{c'} n_a
 \end{aligned}$$

7 where n_c and $n_{c'}$ are the moles of cations, n_a are the moles of anions, and I is the ionic
 8 strength as defined in Eq. (27). $B_{k,i}(I)$ (kg mol^{-1}) and $B_{c,a}(I)$ (kg mol^{-1}) are ionic strength
 9 dependent binary interaction coefficients between solvent main groups and ions, and between
 10 cations and anions, respectively. $C_{c,a}(I)$ ($\text{kg}^2 \text{mol}^{-2}$) are interaction coefficients between
 11 cation \leftrightarrow anion pairs with respect to the total charge concentration. The coefficients
 12 $R_{c,c'}(I)$ (kg mol^{-1}) and $Q_{c,c',a}(I)$ ($\text{kg}^2 \text{mol}^{-2}$) are defined as binary and ternary interactions
 13 involving two different cations. These binary and ternary interaction coefficients have been
 14 introduced in AIOMFAC to improve the description of various ion combinations, specifically
 15 at high ionic strength. Hence, these two terms in Eq. (30) can be vanished or neglected in
 16 other cases, i.e. for low to moderate ionic strengths.

17 In the current approach, the MR terms of activity coefficients for the species and organic
 18 functional groups described in AIOMFAC are estimated using Eq. (30). As mentioned earlier,
 19 the first three interaction coefficients in Eq. (30) are parameterized as functions of ionic

1 strength I , which are similar to the ones used for the Pitzer model of Knopf et al. (2003):

$$2 \quad B_{k,i}(I) = b_{k,i}^{(1)} + b_{k,i}^{(2)} \exp(-b_{k,i}^{(3)} \sqrt{I}), \quad (31)$$

$$3 \quad B_{c,a}(I) = b_{c,a}^{(1)} + b_{c,a}^{(2)} \exp(-b_{c,a}^{(3)} \sqrt{I}), \quad (32)$$

$$4 \quad C_{c,a}(I) = c_{c,a}^{(1)} \exp(-c_{c,a}^{(2)} \sqrt{I}), \quad (33)$$

5 where $b_{k,i}^{(1)}, b_{k,i}^{(2)}, b_{c,a}^{(1)}, b_{c,a}^{(2)}, c_{c,a}^{(1)}$ and $c_{c,a}^{(2)}$ are adjustable parameters, which are determined by
6 fitting AIOMFAC activity coefficients to experimental data sets (see Zuend et al. (2008) for
7 further details). The parameter $b_{c,a}^{(3)}$ was used mostly to describe aqueous salt solutions
8 assuming a fixed value of $0.8 \text{ kg}^{1/2} \text{ mol}^{1/2}$. Similarly, we have considered the same value for
9 the ions when the activity coefficients are estimated from AIOMFAC. Furthermore, Zuend et
10 al. (2008) argued that for such cases, where this value did not result in a satisfactory data fit,
11 $b_{c,a}^{(3)}$ allow to vary. On the other hand, the parameter $b_{k,i}^{(3)}$ was fixed for all mixed organic-
12 inorganic solutions assuming a value of $1.2 \text{ kg}^{1/2} \text{ mol}^{1/2}$. All interaction coefficients in the MR
13 part are symmetric $B_{c,a}(I) = B_{a,c}(I)$. Subsequently, water is defined as the reference solvent
14 for inorganic ions, no explicit ion \leftrightarrow water interactions are determined, i.e., $B_{k=\text{H}_2\text{O},i}(I)$ is
15 prescribed as zero for all inorganic ions. However, the effects of solution non-ideality from
16 cations and anions interacting with water molecules are indirectly accounted for via the cation
17 \leftrightarrow anion interaction coefficients, $B_{c,a}(I)$, $C_{c,a}(I)$, $R_{c,c'}$ and $Q_{c,c',a}$ as the corresponding
18 interaction parameters, that were determined on the basis of (organic-free) aqueous electrolyte
19 solutions.

20 As depicted earlier, the MR interaction parameters in AIOMFAC were fitted for limited
21 organic compounds (i.e. alkyl and hydroxyl) and ions. Contrary, interaction parameters were
22 not evenly available for over all systems of current interest, i.e. to treat the organic
23 compounds and ions involved in multiphase mechanism such as CAPRAM. Hence, in this
24 study, the ion \leftrightarrow ion and organic main group \leftrightarrow ion interaction parameter database is
25 extended by incorporating parameters of the modified LIFAC approach of Kiepe et al. (2006).
26 The complete procedure of the extension of model interaction parameters is explained in
27 Appendix A.1.

1 2.3.4 The short-range contribution

2 The SR contribution $\ln\gamma_{SR}^{ex}$ to the total Gibbs excess energy in SpactMod is represented by the
3 modified group-contribution method UNIFAC (Fredenslund et al., 1975), as performed by
4 Zuend et al. (2008). AIOMFAC incorporates the revised parameter set of Hansen et al. (1991)
5 (standard UNIFAC) for most of the functional group interactions. Besides, these
6 modifications include the insertion of further inorganic ions to account for their effects on the
7 thermodynamic properties such as entropy and enthalpy of mixing apart from their charge-
8 related interactions (Li et al., 1994; Yan et al., 1999; Zuend et al., 2008). AIOMFAC utilizes
9 the specific UNIFAC parameterizations of Marcolli and Peter (2005) for hydroxyl and alkyl
10 functional groups.

11 Similar to the addition of interaction parameters derived for MR part, the same functional
12 groups are also included in the SR part, while maintaining the compatibility with the
13 mathematical model expressions proposed in AIOMFAC. As Zuend et al. (2008), we used the
14 UNIFAC parameterizations of Marcolli and Peter (2005), which are adopted from Hansen et
15 al. (1991). Additionally, the revised parameterizations for the functional group COOH are
16 taken from Peng et al. (2001), which differs from the parameter matrix proposed in standard
17 UNIFAC by Hansen et al. (1991). Since the same mathematical formulations are used in these
18 models and differs only in main group interaction parameters, the parameter matrix is
19 compatible to use. The influence of estimated activity coefficients when merging specific
20 parameters from the distinctive UNIFAC parameterizations within SpactMod has been tested.
21 Sensitivity studies have shown, that SpactMod predict relatively better results when
22 combining the main functional group interaction parameters instead of using the standard
23 UNIFAC parameter set only (see Sect. 3.2). The interaction parameters for these organic
24 functional groups are shown in Appendix B.

25 In UNIFAC, the activity coefficient γ_j of a molecular component j (j can be used for solute
26 or solvent) in a multicomponent mixture is in general expressed as the summation of
27 contributions of (i) a combinatorial part (C) accounting for the geometrical properties of the
28 molecule and (ii) a residual part (R), which results from inter-molecular interactions:

$$29 \ln\gamma_j^{SR} = \ln\gamma_j^C + \ln\gamma_j^R. \quad (34)$$

30 Since ions are treated such as solvent components in the SR terms, resulting activity
31 coefficients in Eq. (34) are with respect to the symmetrical convention on mole fraction basis.

1 For ions, the unsymmetrical normalized activity coefficient is determined from:

$$2 \ln \gamma_i^{SR,(x),\infty} = \ln \gamma_i^{SR,(x)} + \ln \gamma_i^{SR,(x),ref}. \quad (35)$$

3 The symmetrically normalized value at the reference state is computed from the combinatorial
4 and residual parts, by introducing the reference state conditions of the ions (setting

5 $x_w = 1, \sum_s x_s = 0$ for $s \neq w$ and $\sum_i x_i = 0$):

$$6 \ln \gamma_i^{SR,(x),ref} = \ln \frac{r_i}{r_w} + 1 - \frac{r_i}{r_w} \\ + \frac{z}{2} q_i \left[\ln \left(\frac{r_w q_i}{r_i q_w} \right) - 1 + \frac{r_w q_i}{r_i q_w} \right] \\ + q_i \left(1 - \ln \psi_{w,i} - \psi_{i,w} \right), \quad (36)$$

7 where subscript w stands for the reference solvent (water). The parameters q_i and r_i represent
8 the surface area and the volume, respectively, of component i . The last term on the right-hand
9 side of Eq. (36) reflects the residual part reference contribution and becomes zero as we
10 defined the SR ion \leftrightarrow solvent interactions to be zero. Fig. 4 shows the binary species
11 combinations, for which the specific parameters have been used in this study. Mean
12 interactions between ions and water are indirectly represented by the parameters of the cation
13 \leftrightarrow anion interaction pairs according to (Zuend et al., 2008), since the aqueous solution is
14 defined as the reference system similar to the assumption used in conventional Pitzer models
15 (Pitzer, 1991). The relative van der Waals subgroup volume and surface area parameters, R_i
16 and Q_i , account for pure component properties. At the same time, R_i and Q_i values for the
17 ions can be estimated from the ionic radii. In order to maintain the compatibility with the
18 model equations of AIOMFAC, the hydrated group volume and surface area parameters R_i^H
19 and Q_i^H are calculated using an empirical parameterization given by Achard et al. (1994). For
20 those ions, the activity coefficients are estimated using the mod. LIFAC approach. Likewise,
21 the database is extended for other ions in order to estimate the activity coefficients from the
22 SR part. The measured apparent dynamic hydration numbers (N_i^{ADH}) data are adopted from
23 Kiriukhin and Collins (2002) to estimate the final values R_i^H and Q_i^H instead of R_i and Q_i .
24 R_i^H and Q_i^H are computed consistently in the model equations (see Table A2 in the Appendix)
25 by:

$$26 R_i^H = R_i + N_i^{ADH} \cdot R_w, \quad (37)$$

$$Q_i^H = Q_i + N_i^{ADH} \cdot Q_w, \quad (38)$$

where R_w and Q_w refer to the values of the water molecule and N_i^{ADH} are measured apparent dynamic hydration numbers at 303.15 K (Kiriukhin and Collins, 2002). As shown in Fig. 4, the interactions of the ions Mg^{2+} , Ca^{2+} , F^- , I^- , OH^- , NO_2^- , CO_3^- and CH_3COO^- are implemented from Kiepe et al. (2006). Due to the increasing interest on remaining ions included in the multiphase mechanism CAPRAM (e.g. Fe^{2+} , succinate, and malonate) the activity coefficients are computed while prescribing the corresponding interaction parameters as zero.

2.3.5 Total activity coefficients

Finally, SPACCIM's activity coefficient module (SpactMod) estimates the total activity coefficients for each species according to the Gibbs energy (cp. Eqs. (22) and (24)). Then, the activity coefficient of a solvent species s is determined by Li et al. (1994); Yan et al. (1999); Kiepe et al. (2006); Zuend et al. (2008)

$$\ln \gamma_s^{(x)} = \ln \gamma_s^{LR,(x)} + \ln \gamma_s^{MR,(x)} + \ln \gamma_s^{SR,(x)} \quad (39)$$

Accordingly, the complete expression for the ions, with regard to the unsymmetrical convention on molality basis at which the standard state is the hypothetical ideal solution of unit molality at system pressure and temperature, can be written as follows:

$$\ln \gamma_i^{(m)} = \left[\ln \gamma_i^{LR,(x),\infty} + \ln \gamma_i^{MR,(x),\infty} + \ln \gamma_i^{SR,(x),\infty} \right] - \ln \left[\frac{M_w}{\sum_s x_s^* M_s} \right] + M_w \sum_{i'} m_{i'} \quad (40)$$

where M_s is the molar mass of solvent component s , x_s^* its salt-free mole fraction, and $m_{i'}$ is the molality of ion i' . The last term on the right-hand side of Eq. (40) converts the activity coefficient $\ln \gamma_s^{(x)}$ (infinitely diluted reference state on the mole fraction basis) to the activity coefficient on molality basis and infinitely diluted (in water) reference state. One can derive this term based on convention-independence of the chemical potentials $\left(\mu_i^{(m)}(p,T,n_j) = \mu_i^{(x)}(p,T,n_j) \right)$ and the definitions of the chosen reference states (Zuend et al., 2008).

The extension of database by the combination of AIOMFAC and modified LIFAC makes

1 SPACCIM a versatile tool to study the influence of the treatment of solution non-ideality on
2 multiphase aerosol chemistry. SpactMod is highly flexible to extension and further inclusion
3 of organic functional groups and ions, whenever the required data become available. During
4 the implementation of the code, the activity coefficients responsible for LR and SR
5 contribution terms are computed for all the ions (either cation or anion) included in the
6 considered chemical system. For those species, where the interaction parameters are not
7 available to compute MR contribution terms; they are prescribed as unity (i.e., $\gamma_i^{MR,(x),\infty} = 1$)
8 due to the lack of extensive database.

9 **3 Model evaluation and applications**

10 In this section we will examine the model extensions described above. Especially, the activity
11 coefficient module SpactMod is evaluated and compared with literature data. The reliability
12 of the extended SPACCIM code is shown in the last subsection. Furthermore, the deviation of
13 the activity coefficients from ideality and, consequently, the impact on the chemical behavior
14 are demonstrated for a test scenario. A more detailed analysis of the impact of the non-ideality
15 approach on the multiphase will be published in a separate paper.

16 **3.1 Evaluation of the activity coefficient module**

17 Considerable effort has been devoted by several authors (see e.g., Raatikainen and Laaksonen
18 (2005); Tong et al. (2008); Zuend et al. (2008)) to compare different established activity
19 coefficient models that could be potentially suitable for modeling of hygroscopic properties of
20 organic-electrolyte particles as well as the prediction of activity coefficients of aqueous
21 species. The investigations summarized here were aimed to evaluate the robustness of the
22 implemented module SpactMod and to check the reproducibility towards original model
23 results. However, the interaction parameters in the applied models were fitted against
24 measurements. Hence, this comparison can be considered as indirect comparison with
25 measurements. Furthermore, results are also compared with direct also water activity
26 measurements and the AIM model (Aerosol Inorganic Model) of Clegg et al. (1998b, 1998a).
27 The model comparisons cover a scale, ranging from very simple to complex simulations.
28 Initially, the comparison is performed for selected binary aqueous electrolyte solutions, then
29 aqueous organic solutions, followed by mixtures of aqueous organic-electrolyte solutions.
30 However, here we present the results of selected examples only.

1 3.1.1 Comparison between activity coefficient models for inorganic systems

2 Naturally, the reproducibility of the original AIOMFAC results in Zuend et al. (2008) was
3 verified in a first step. Note that the graphs of the newly implemented module SpactMod
4 depicted in Figs. 5 and 6 correspond to the original results given in Zuend et al. (2008). Fig. 5
5 shows the comparison between calculated water activities predicted by the selected four
6 models and experimental data. The differences for the electrolyte mixture of NaCl + NH₄NO₃
7 are in good agreement up to moderate salt concentrations ($x_w \geq 0.5$). The values for high
8 concentrations ($x_w \leq 0.4$) indicate the formation of a solid salt (or hydrate), when the solution
9 becomes supersaturated as well as the deliquescent point of the particular salt. The models do
10 not reproduce this, since the formation of solids was not incorporated in the present model
11 calculations. As can be seen from Figs. 5 and 6, the modeled water activities agree well with
12 each other at low concentrations. Contrary at high salt concentrations, mod. LIFAC strongly
13 deviates from SpactMod as shown in Fig. 5, by a steep increase in a_w and in Fig. 6 by an
14 increase followed by a sharp decrease, as shown by Zuend et al. (2008). Note that the
15 Ca(NO₃)₂ parameterization of mod. LIFAC (see Fig. 6) results only from water activity data
16 of bulk measurements as the approach of Ming and Russell (2002) model, behaves similar to
17 SpactMod at medium concentrations and proceed to formation of solids. The interaction
18 coefficients of AIOMFAC applied in SpactMod were fitted from vapor-liquid as well as
19 liquid-liquid equilibrium data, salt solubilities and electromotive force measurements
20 covering also high solution concentrations and ternary mixtures (Zuend et al., 2008). Hence,
21 the slope of the curve enables much better descriptions and predictions up to high
22 concentrations, even very low water concentration available and at high ionic strength. It is
23 noted that Ca(NO₃)₂ is not available in the AIM, thus Fig. 6 includes only results of the other
24 activity coefficient approaches.

25 Apart from the predicted water activities, the calculated mean activity coefficients also have
26 differences with each other. Therefore, a comparison of mean activity coefficients is
27 presented additionally in Fig. 6. The mean activity coefficient (γ_{\pm}) is related to single ion-
28 activity coefficients by

$$29 \quad \gamma_{\pm} = (\gamma_+^{V_+} \cdot \gamma_-^{V_-})^{1/(V_+ + V_-)} \quad (41)$$

30 where γ_+ and γ_- are the activity coefficients of a cation and anion, respectively. V_+ and V_- are
31 the corresponding stoichiometric coefficients. The mean activity coefficients predicted by

1 AIOMFAC and the approach of Ming and Russell (2002) show a similar curve shape with
2 5 % of difference. In contrast, mod. LIFAC shows a different behavior especially for water
3 fractions later than 0.8.

4 3.1.2 Verification of SpactMod for organic-electrolyte mixtures

5 In this section, the performance of different activity coefficient models is evaluated by
6 comparing calculated and measured water activities of mixtures of electrolyte and organic
7 system. For all water activity calculations, the organic acids are treated as non-dissociating
8 solutes, and a single liquid phase is assumed with no solid phases present. All calculations are
9 performed at atmospheric pressure (1 atm) and at 298 K.

10 Fig. 7 shows the comparison of experimental data with predicted water activities using
11 different UNIFAC parameterizations. Here, the parameters for the original UNIFAC are
12 adopted from Hansen et al. (1991). Furthermore, a revised set of fitted UNIFAC parameters
13 given by Peng et al. (2001) for the interactions of functional groups OH, H₂O and COOH is
14 used for the comparison. As depicted in Fig. 7, the original UNIFAC and Ming and Russell
15 (2002) exhibit similar behavior for all water fractions. Moreover, SpactMod and the version
16 of Peng et al. (2001) have deviations that are usually less than 50% of the deviations with the
17 original UNIFAC. Furthermore, the original UNIFAC exhibits much bigger deviations than
18 the UNIFAC version of Peng et al. (2001) and SpactMod. The last two models show a similar
19 behavior and a good agreement with the measurements. In difference to the Peng approach,
20 SpactMod take into account dynamic hydration numbers (see Eq. (37) and (39)), which is in
21 consistency with the computation of the combinatorial term in AIOMFAC.

22 Fig. 8 shows the comparison of mean ionic activity coefficients of binary electrolyte mixtures.
23 As can be seen from the plot, good results were obtained by SpactMod based on mod. LIFAC
24 parameterization. Mod.LIFAC shows better results compared to LIFAC due to the improved
25 reference state calculation of ions in the SR part. Due to the normalization of ions, SpactMod
26 gives better agreement compared to original LIFAC for these binary electrolytes.

27 Fig. 9 shows the comparison between predicted water activities from different activity
28 coefficient models for the mixture of (NH₄)₂SO₄ + Glycerol + H₂O [(2:1:1) mole ratio]. As
29 expected, SpactMod accurately reproduces the results from the original AIOMFAC. All the
30 models behave similarly up to moderate concentrations ($x_w = 0.6$). As in Fig. 6, at lower water
31 activity, mod. LIFAC and LIFAC strongly deviate from SpactMod. As argued earlier, LIFAC

1 and mod. LIFAC are able to predict vapor liquid equilibria and liquid liquid equilibria but
2 cannot describe the deviations from ideality at high concentrations. A steep increase of a_w
3 shown in Fig. 9 have to be rated as artefacts of the LIFAC and mod. LIFAC parameterization.
4 Fig. 10 shows the comparison between experimental and predicted water activities for the
5 mixture of $(\text{NH}_4)_2\text{SO}_4$ + Ethanol + Acetic acid [(2:1:1) mole ratio]. All the models strongly
6 agree with the measurements at high relative humidities or at low and moderate salt
7 concentrations ($x_w \approx 0.8$). However at the deliquescent phase ($x_w \approx 0.6$), the mod. LIFAC
8 and Ming and Russell (2002) model strongly deviate from SpactMod. These differences for
9 lower water fractions are mainly caused by the different treatment of ion \leftrightarrow organic
10 interactions included in the models. It can be seen from Fig. 10 that the strange behavior does
11 not appear for the pure organic and pure electrolyte mixture predictions. The MR interaction
12 term in the model is responsible for this atypical shape in the predictions. Moreover,
13 Raatikainen and Laaksonen (2005) argued that, in the MR part, the logarithms of activity
14 coefficients are calculated as sums of terms, which are proportional to the fitting parameters,
15 ion molalities and ionic strength. Because these terms have quite large numerical values, and
16 a small change in the interaction parameters or molality can cause a very big change to
17 activity coefficients. The MR part and modification of SR part given in SpactMod could be
18 the main reason, since this model can predict the water activities at high salt concentrations as
19 well. Consequently, as can be seen from Fig. 10, mod. LIFAC have an increase followed by a
20 sharp decrease, features that have to be rated as artifacts of the mod. LIFAC parameterization,
21 whereas the Ming and Russell (2002) model has also a strong increase after the water fraction
22 is about ($x_w \approx 0.3$). As mentioned earlier, these artifacts indicate the formation of a solid salt
23 (or hydrate), when the solution becomes supersaturated, since the formation of solids was not
24 enabled in the model calculations.

25

26 However, the consideration here is only a limited set of mixtures of organic-electrolyte
27 compounds. Hence, the presented results should be viewed as a first assessment. The scarcity
28 of experimental data for mixtures of atmospheric relevance remains a limitation for testing
29 activity coefficient models. When experimental data become available in the future, the
30 models can be validated against measurements, while comparing the water activity and
31 species activity coefficients against water fraction x_w . All in all, despite the difficulties in
32 determining the ion \leftrightarrow organic mixture parameters, it should be noted that the ion \leftrightarrow organic

1 interaction parameters have improved the model performance, a fact which was already noted
2 in previous studies (Clegg and Seinfeld, 2006b, a; Clegg et al., 2001; Tong et al., 2008)

3 **3.2 Sensitivity studies on the importance of the different interactions**

4 Tong et al. (2008) studied the importance of inclusion of a treatment of ion ↔ organic
5 interactions and states that these interactions would substantially improve the performance of
6 the coupled models over that of the decoupled models. It has been concluded that, decoupled
7 approaches, such as those in CSB (Clegg et al., 2001), ADDEM (Topping et al., 2005a, b),
8 performs well, and in some cases better than the coupled models (Ming and Russell, 2002;
9 Erdakos et al., 2006a, b). Additionally in such cases, the ion ↔ organic terms do not
10 necessarily lead to improved model predictions. At the same time, models are prerequisite,
11 composed of an aqueous electrolyte term, an (aqueous) organic term, and an organic ↔ ion
12 mixing term in order to treat the organic-inorganic mixtures. In contrast to the study of Tong
13 et al. (2008), the present study aims at the evaluation of the importance of different interaction
14 terms in the model approach Eq. (24) for the computation of water activities and the activity
15 coefficients.

16 Intermolecular forces or interactions are essential in the deliquesced particle phase, where
17 high solute concentrations and low water fractions are available. They are important because
18 they are responsible for many of the physical properties of solids, liquids, and gases.
19 Moreover, these interaction forces become significant at the molecular range of about
20 1 nanometer or less, but are much weaker than the forces associated with chemical bonding.
21 The characteristic contribution of different interaction forces from the model development
22 point of view in the solution can be computed using Eq. (24). Utilizing this conceptual idea in
23 the computation of activity coefficients, here we address the question, which intermolecular
24 forces of attraction are important and need be considered for the treatment of solution non-
25 ideality for organic-electrolyte mixtures. In order to answer this question, the SpactMod is
26 used for sensitivity studies. Overall, the studies have revealed that middle-range (MR)
27 interactions are important to compute the total activity coefficients.

28 Fig. 11 shows the contribution of different interaction forces in the solution for the mixture of
29 NaCl + (NH₄)₂ SO₄ + Ethanol + Malonic acid [1:1:1:1 (mole ratio)] as an example. However,
30 the deviations regarding the different interactions depend on the considered mixture. As can
31 be seen in Fig. 9, the water activity strongly deviates in absence of MR interaction forces,

1 mainly caused from ion ↔ ion, ion ↔ dipole and ion ↔ induced dipole forces. Thus, the MR
2 interactions were found important. Similar to the findings of Tong et al. (2008), it is expected
3 that ion ↔ organic interactions be of most importance in solutions with high solute
4 concentrations, for which inclusion of ion ↔ organic parameters would be beneficial.
5 However, the absence of each interaction terms can be seen in Fig. 11. The short-range
6 interactions also influence in the total contribution of computation of water activity, where the
7 deviations are about 10%. In the case of considered the MR and SR interactions, the
8 deviations are about 25%. It should be noted that the ion ↔ organic interactions are the
9 dominant interaction forces in the solution, however the further interaction forces need to be
10 considered. The deviations from the total contribution of interaction forces is significant in all
11 ranges of relative humidity as well as in the full range of concentration. Nevertheless, the
12 deviations are increasing from lower salt/acid concentration to higher. During the low
13 salt/acid concentration ($x_w \approx 0.9$) the contribution of the considered interactions were found
14 similar.

15 **3.3 First application of the advanced SPACCIM model**

16 To demonstrate the functioning of the whole advanced SPACCIM model framework
17 including the newly considered activity coefficient module SpactMod and a complex
18 multiphase aerosol chemistry mechanism, first air parcel simulations have been performed
19 with a simple model scenario. In the two following subsections, the applied model scenario
20 and chemical mechanism is briefly outlined, and subsequently selected model results are
21 presented. However, it is noted that the presented simulations are not aimed at the detailed
22 examination of non-ideal solution effects on multiphase chemical processes. The detailed
23 investigation of this complex issue will be given in a companion paper (Rusumdar et al.,
24 2015).

25 **3.3.1 Model scenario and chemical mechanism**

26 In the applied meteorological scenario, an air parcel moves along a predefined 3-hour model
27 trajectory that involves three cloud passages and non-cloud periods in which the aerosol
28 particles are deliquesced. Simulations were performed with and without consideration of non-
29 ideal solutions. Furthermore, the simulations have been performed with two different relative
30 humidity levels (90 % r.h. and 70% r.h.) during the non-cloud periods. In total, simulations
31 have been performed for four cases: with and without consideration of non-ideal solutions and

1 both with a 90% and 70% relative humidity level during the non-cloud periods, respectively.
2 For the modeling, mono-disperse aerosol particles with a radius of 200 nm and a number
3 concentration of $1.0 \cdot 10^{+8} \text{ cm}^{-3}$ were used.

4 For the test simulations, a complex multiphase chemistry mechanism has been applied. The
5 applied mechanism consists of the gas phase mechanism RACM-MIM2ext (Tilgner and
6 Herrmann, 2010) and an extended version of the aqueous phase mechanism CAPRAM2.4
7 (CAPRAM2.4 + organicExt). The employed aqueous phase mechanism consists of the
8 CAPRAM2.4 mechanism (Ervens et al., 2003) combined with the reduced organic extension
9 of CAPRAM3.0i-red (Deguillaume et al., 2010) along with the condensed oxidation scheme
10 of malonic acid and succinic acid based on the CAPRAM3.0i-red (see Deguillaume et al.
11 (2010) for further details). Thus, the aqueous phase mechanism contains a detailed oxidation
12 scheme of inorganic as well as organic compounds with 204 species and 477 reactions. In the
13 considered organic reaction scheme describes the chemistry of organic compounds with up to
14 4 carbon atoms and different functional groups. All model simulations have been performed
15 for continental remote environmental conditions (see Ervens et al. (2003) for further details).

16 3.3.2 Model results

17 *Modeled activity coefficients of key inorganic ions*

18 Fig. 12 depicts the time evolution of the activity coefficients of main inorganic ions and key
19 transition metal ions (TMIs) modeled for the two different relative humidity cases. The plots
20 show, expectedly, a strong dependency on the microphysical conditions. During cloud
21 conditions, the modeled activity coefficients are almost equal to unity for the depicted ions.
22 The in-cloud activity coefficients of ions with charge state 3+ deviate a bit more from the one
23 than less charged ions. Under concentrated deliquesced particle conditions, the activity
24 coefficients of ions are much lower and show a strong dependence on the relative humidity
25 level. In the 90% r.h. case, the activity coefficients of singly charged ions are in the range of
26 0.6-0.7, whereas the modeled coefficients for the doubly and triply charged ions are 0.3-0.35
27 and 0.1, respectively. Additionally, Fig. 12 reveals that the deviations from ideal behavior
28 strongly depend on the species regarded but mainly on the charge state. The comparison with
29 the 70% r.h. case shows clearly that the activity coefficients do not change linearly with
30 relative humidity. This fact is caused by a non-linear change of activity coefficients in terms
31 of the molality due to the different types of interactions in the solution. From Fig. 10 it can be

1 seen that the activity coefficients of singly or doubly charged ions are significantly lowered in
2 the 70% r.h. case compared to the 90% r.h. case. However, no substantial decrease is
3 simulated for triply charged ions such as Fe^{3+} , which are still in the range of 0.1. Interestingly,
4 the activity coefficient of H^+ show only a drop of 0.1 between the two cases, while the activity
5 coefficients of other singly charged ions are lowered by approximately 0.2.

6 In total, the simulated activity coefficients of inorganic ions with values below 1 implicate
7 that the mass fluxes of chemical processes in deliquesced particles involving those ions are
8 most likely decreased leading thus to a different chemical regime than present under ideal
9 cloud conditions. For example, the huge differences in the activity coefficients of the TMIs
10 can lead to substantial differences in the redox cycling.

11

12 *Modeled activity coefficients of important organic compounds*

13 Fig. 13 illustrates the modeled time evolution of the activity coefficients of important organic
14 carbonyl compounds and organic acids (both free acid and anions) for the two different
15 relative humidity cases. For organic carbonyl compounds, the depiction reveals quite uneven
16 pattern. For hydrated glyoxal and glycolaldehyde, the predicted activity coefficient are larger
17 than 1 in both model cases. In contrast, activity coefficients below 1 are predicted for the
18 other unhydrated organic carbonyls and the hydrated formaldehyde. As shown for the organic
19 ions, there is a strong dependence of the non-ideal behavior on the species and their specific
20 forms (i.e., functional groups included) as well as additionally the relative humidity
21 conditions. For the hydrated glyoxal and glycolaldehyde with more than 3 OH functionalities
22 included, activity coefficient values of about 1.2 and 1.6, respectively, are modeled in the
23 90% r.h. case. Many times higher activity coefficients are calculated for the 70% r.h. case.

24 The predicted activity coefficients of the organic acid anions behave similarly to the inorganic
25 ions. Differences can be observed for the 2 free acids plotted in Fig. 13. While the activity
26 coefficient of formic and acetic acid corresponds mainly to the present supersaturation of 0.9
27 in the 90% r.h. case, the activity coefficient of acetic acid are higher during the more
28 concentrated case at 70% r.h. This behavior is caused by the additional methyl group. In
29 summary, the predicted activity coefficients of organic compounds imply that the chemical
30 processing of organics can be either increased or decreased under deliquesced particle
31 conditions depending on the particular compound.

1

2 *Modeled acidity*

3 The modeled pH-values for the four different simulations are plotted in Fig. 14. The pH
4 values simulated with and without consideration of non-ideal solution effects reveal no
5 difference during the cloud periods but substantial deviations during the non-cloud periods.
6 During the cloud periods under almost ideal conditions, an decrease of the pH value is
7 modeled due to occurring acidifying reactions such as the S(IV) to S(VI) conversion. The
8 acidification is strongest during the first cloud passage and lower during the two following
9 clouds. From the two plots, it can be seen that the difference between the ideal and non-ideal
10 case is somewhat larger for the 70% case. On average, the pH values of the simulations
11 considering solution non-ideality are -0.27 and -0.44 pH units lower under 90% r.h. and
12 70% r.h. conditions, respectively. This, lower acidity in the non-ideal case is able to affect
13 both aqueous phase chemical reactions (i.e., acid catalyzed reactions) and all dissociations.
14 Further implications of this difference for the chemical processing are not discussed here, but
15 outlined in a companion paper (Rusumdar et al., 2015).

16 Overall, the performed simulations demonstrated that the further developed SPACCIM model
17 performs well and the simulation results emphasize the consideration of solution non-ideality
18 in multiphase chemistry models especially for an adequate description of the chemical aerosol
19 processing in deliquesced particles.

20

21 **4 Summary**

22 In the present work, a robust and comprehensive model framework is developed and
23 implemented in order to treat the aqueous phase chemistry considering non-ideal solution
24 effects in the context of the multiphase model SPACCIM. The implemented group-
25 contribution concept enables the reliable estimation of activity coefficients for organic-
26 inorganic mixtures composed of various ions and functional groups. Treatment of solution
27 non-ideality for mixed-solvent systems requires a careful combination of standard-state
28 properties with activity coefficient models. This was achieved in practice by ensuring the
29 correct representation of Gibbs excess energy by three contributions to the excess Gibbs
30 energy. Surface tension depreciation due to the organic compounds is effectively accounted
31 and included in the model framework. Interaction parameters accounts for various

1 contributions of interactions. Mixed organic-inorganic systems from the literature are
2 critically assessed and a new database is created. For all tested types of systems and data, the
3 designed model SpactMod has been shown to reproduce both the original model results and
4 experimental results with good accuracy. Sensitivity studies have shown that the inclusion of
5 middle-range interaction contributions is necessary. This inclusion enhances the robustness of
6 the model. The current developed framework is open to extension to further organic
7 functional groups, and ions, when thermodynamic data on such systems become available.
8 Indeed, compound specific parameter, such as charge, organic functional groups and
9 interaction parameters, required for the activity coefficient model as well as chemical reaction
10 data are read from input files. The interaction parameters will be easily incorporate and the
11 database can flexibly updated. Besides, the computer code will facilitate the changes and
12 future inclusions. The implemented numerical schemes merely give good computational
13 efficiency. Due to the limitations regarding the lack of experimental data, and the ability to
14 treat the organic-electrolyte mixtures of atmospheric relevance at various complexities,
15 predictions are improved considerably while using extended interaction parameters. In future,
16 the database will be extended with new parameters of recent studies ((Zuend et al., 2011;
17 Mohs and Gmehling, 2013; Ganbavale et al., 2015) within this activity coefficient module.
18 First test simulations with the advanced SPACCIM model have demonstrated the applicability
19 of SpactMod within the model framework. Furthermore, the simulations emphasize that the
20 treatment of solution non-ideality is mandatory for modeling multiphase chemistry processes
21 in deliquesced particles. For important ions, the model runs have shown activity coefficients
22 <1 and a strong dependency on the charge state as well as on the microphysical conditions.
23 Thus, the model results implicate that the chemical processing of ions in deliquesced particles
24 is potentially lowered and different to a chemical regime present under ideal cloud conditions.
25 For organic compounds, the modeled activity coefficients the activity coefficients are both
26 lower and higher than unity suggesting that the chemical processing of organics can be either
27 increased or decreased under deliquesced particle conditions depending on the particular
28 species. The complexity of consideration of non-ideal solutions and its influence on
29 multiphase chemistry is investigated in detail in a companion paper (Rusumdar et al., 2015).

30

1 Appendix A: SPACCM's activity coefficient module

2 A.1 Middle-range contribution-model extension

3 The activity coefficients responsible for the MR interaction forces are obtained by
 4 differentiating the Eq. (30) with respect to the number of moles of solvent main groups,
 5 cations, and anions respectively. Thus, expressions for a specific cation c^* on a mole fraction
 6 basis can be written as:

$$\begin{aligned}
 \ln \gamma_{c^*}^{MR, (x), \infty} = & \frac{1}{M_{av}} \sum_k B_{k, c^*}(I) x'_k + \frac{z_{c^*}^2}{2M_{av}} \sum_k \sum_i B'_{k, i}(I) x'_k m_i + \sum_a B_{c^*, a}(I) m_a \\
 & + \frac{z_{c^*}^2}{2} \sum_c \sum_a B'_{c, a}(I) m_c m_a + \sum_a C_{c^*, a}(I) m_a \sum_i m_i |z_i| \\
 & + \sum_c \sum_a \left[C_{c, a}(I) |z_{c^*}| + C'_{c, a}(I) \frac{z_{c^*}^2}{2} \sum_i m_i |z_i| \right] m_c m_a \\
 & + \sum_c R_{c^*, c} m_c + \sum_c \sum_a Q_{c, c^*, a} m_c m_a
 \end{aligned} \tag{A1}$$

8 For a better understanding, Eq. (A1) can be divided into different terms:

$$\ln \gamma_i^{MR} = T_i^{solvent} + T_i^{ion-solvent} + T_i^{ion} + T_i^{ion-ion} + T_i^{ternary} \tag{A2}$$

10 with

$$T_i^{solvent} = \frac{1}{M_{av}} \sum_k B_{k, c^*}(I) x'_k, \tag{A3}$$

$$T_i^{solvent} = \frac{1}{M_{av}} \sum_k B_{k, c^*}(I) x'_k, \tag{A4}$$

$$T_i^{ion} = \sum_a B_{c^*, a}(I) m_a + \sum_c R_{c^*, c} m_c + \sum_a C_{c^*, a}(I) m_a \sum_i m_i |z_i|, \tag{A5}$$

$$\begin{aligned}
 T_i^{ion-ion} = & \frac{z_{c^*}^2}{2} \sum_c \sum_a B'_{c, a}(I) m_c m_a \\
 & + \sum_c \sum_a \left[C_{c, a}(I) |z_{c^*}| + C'_{c, a}(I) \frac{z_{c^*}^2}{2} \sum_i m_i |z_i| \right] m_c m_a,
 \end{aligned} \tag{A6}$$

$$T_i^{ternary} = \sum_c \sum_a Q_{c, c^*, a} m_c m_a. \tag{A7}$$

16

1 The term $T^{ternary}$ stands for the ternary terms in Eq. (30) which was incorporated by Zuend et
 2 al. (2008) to improve the treatment of systems at high ionic strength.

3
 4 As mentioned in Sect. 3, the activity coefficient module SpactMod is substantially based on
 5 AIOMFAC (Zuend et al., 2008). But it has been extended by including the new interaction
 6 parameters for the species shown in Fig. 4, based on mod. LIFAC (Kiepe et al., 2006). A
 7 sufficient evaluation was performed using the actual experimental database, which has been
 8 significantly enlarged within the last years (see Raatikainen and Laaksonen (2005); Tong et
 9 al. (2008)).

10
 11 The general concentration dependence of the interaction parameters can be written as
 12 analogous to Eq. (31):

$$14 \quad B_{i,j} = b_{i,j} + c_{i,j} \exp(a_1 \sqrt{I}) \quad (A8)$$

15 where, $b_{i,j}$, $c_{i,j}$ and a_1 are adjustable interaction parameters. However, according to
 16 mod. LIFAC (Kiepe et al., 2006), the second virial coefficient $B_{i,j}$ is the interaction
 17 coefficient between the species i and j . The relations of the ion \leftrightarrow ion interaction parameter
 18 $B_{c,a}$ and ion \leftrightarrow solvent group interaction parameter $B_{k,ion}$ to the ionic strength are described
 19 by Kiepe et al. (2006).

$$21 \quad B_{c,a} = b_{c,a} + c_{c,a} \exp(-\sqrt{I} + 0.125I), \quad (A9)$$

$$22 \quad B_{k,i} = b_{k,i} + c_{k,i} \exp(-1.2\sqrt{I} + 0.25I). \quad (A10)$$

23 The equation for interaction parameters shown in the two versions (Eqs. 31 – 32, A9 and
 24 A10) was compared and the final model equations are derived. As a result, Eq. (A9) can be
 25 written as similar to Eq. (32):

$$26 \quad B_{c,a}(I) = b_{c,a} + c_{c,a} \exp\left(-\left(1.0 - 0.125\sqrt{I}\right)\sqrt{I}\right) \quad (A11)$$

1 Based on this, while using the similar model equations, the database was utilized with the ion
2 \leftrightarrow ion interaction parameters as:

$$3 \quad b_{c,a}^{(1)} = b_{c,a}, \quad b_{c,a}^{(2)} = c_{c,a}, \quad b_{c,a}^{(3)} = (1.0 - 0.125\sqrt{I}). \quad (\text{A12})$$

4 Since ion \leftrightarrow ion \leftrightarrow ion interaction parameters (ternary interactions) were not available with
5 mod. LIFAC, the interaction parameters for $c_{c,a}^{(1)}$ and $c_{c,a}^{(2)}$ were assigned to zero. Similar to ion
6 \leftrightarrow ion interaction parameters, the model equations to compute the solvent \leftrightarrow ion interaction
7 parameters were also modified. Compared to Eq. (31) and Eq. (A10), the parameters are
8 assigned as:

$$9 \quad b_{k,i}^{(1)} = b_{k,i}, \quad b_{k,i}^{(2)} = c_{k,i}, \quad b_{k,i}^{(3)} = (1.2 - 0.125\sqrt{I}). \quad (\text{A13})$$

10 Afterwards without altering the model equations given in AIOMFAC, computation of activity
11 coefficients for all species is performed. Even, the ternary and quaternary interactions were
12 also assigned to zero during the computation of activity coefficients for solvent groups.
13 Hence, the model equations reduced to original model equations as described in [Kiepe et al.](#)
14 [\(2006\)](#) and [Yan et al. \(1999\)](#). Similarly, for the ions, the ternary interactions (Eq. (A6)) are
15 not considered to compute the activity coefficients, which are not explicitly described in the
16 original AIOMFAC. So this term is equal to zero, and hence the Eq. (3.19) and Eq. (3.20)
17 given in [Zuend et al. \(2008\)](#) lead to the original model equations (see Eq. (12) in [Kiepe et al.](#)
18 [\(2006\)](#)). The chemical species included in the multiphase mechanism are categorized by
19 different classes in the input files. While using these input files, this algorithm performs a
20 search, and gathers the information, whether the computation of interaction parameters needs
21 to perform according to AIOMFAC or the modified equations specified according to [Kiepe et](#)
22 [al. \(2006\)](#). Thus, the adjustable interaction parameters are used to compute and finally utilized
23 by the activity coefficients responsible for MR interactions.

24

25

26

1

Table A1: MR Parameters $b_{k,i}^{(1)}$ and $b_{k,i}^{(2)}$ between solvents and ions (AIOMFAC- Black/ mod. LIFAC- Red)

2

| Ion | Group | $b_{k,i}^{(1)}$ (kg mol ⁻¹) | $b_{k,i}^{(2)}$ (kg mol ⁻¹) | Ion | Group | $b_{k,i}^{(1)}$ (kg mol ⁻¹) | $b_{k,i}^{(2)}$ (kg mol ⁻¹) |
|-------------------------------|-----------------|--|--|-------------------------------|-------|--|--|
| Na ⁺ | CH _n | 0.124972 | - 0.031880 | Na ⁺ | OH | 0.080254 | 0.002201 |
| K ⁺ | CH _n | 0.121449 | 0.015499 | K ⁺ | OH | 0.065219 | -0.170779 |
| NH ₄ ⁺ | CH _n | 0.103096 | -0.001083 | NH ₄ ⁺ | OH | 0.039373 | 0.001083 |
| Ca ²⁺ | CH _n | 0.000019 | -0.060807 | Ca ²⁺ | OH | 0.839628 | -0.765776 |
| Mg ²⁺ | CH _n | - 0.34610 | -0.44995 | Mg ²⁺ | OH | 0.281980 | 0.07617 |
| Zn ²⁺ | CH _n | - 0.10163 | - 0.06578 | Zn ²⁺ | OH | 0.036480 | 0.02249 |
| Cl ⁻ | CH _n | 0.014974 | 0.142574 | Cl ⁻ | OH | -0.042460 | -0.128063 |
| NO ₃ ⁻ | CH _n | 0.018368 | 0.669086 | NO ₃ ⁻ | OH | -0.128216 | -0.962408 |
| SO ₄ ²⁻ | CH _n | 0.101044 | -0.070253 | SO ₄ ²⁻ | OH | -0.164709 | 0.574638 |

| | | | | | | | |
|-------------------------------|------------------|-----------|-----------|----------------------------------|--------------------|-----------|-----------|
| I ⁻ | CH _n | 0.01206 | - 0.02777 | I ⁻ | OH | -0.04479 | 0.04151 |
| | | | | F ⁻ | OH | 0.15233 | -0.04145 |
| | | | | CH ₃ COO ⁻ | OH | 0.02672 | -0.02117 |
| Na ⁺ | H ₂ O | 0.00331 | -0.00143 | Na ⁺ | CH ₃ OH | 0.16617 | 0.03928 |
| K ⁺ | H ₂ O | 0.00258 | - 0.00088 | K ⁺ | CH ₃ OH | 0.10797 | 0.19164 |
| NH ₄ ⁺ | H ₂ O | 0.00088 | 0.00288 | NH ₄ ⁺ | CH ₃ OH | 0.20529 | - 0.10550 |
| Ca ²⁺ | H ₂ O | 0.01105 | 0.00641 | Ca ²⁺ | CH ₃ OH | 0.37818 | 0.00247 |
| Mg ²⁺ | H ₂ O | 0.00050 | 0.01163 | Cu ²⁺ | CH ₃ OH | 0.00789 | - 0.06944 |
| Cu ²⁺ | H ₂ O | - 0.00571 | - 0.00760 | Zn ²⁺ | CH ₃ OH | 0.16775 | - 0.44229 |
| Zn ²⁺ | H ₂ O | - 0.01848 | 0.00001 | | | | |
| Cl ⁻ | H ₂ O | -0.00128 | - 0.00020 | Cl ⁻ | CH ₃ OH | - 0.03352 | 0.00242 |
| NO ₃ ⁻ | H ₂ O | 0.03228 | - 0.00083 | NO ₃ ⁻ | CH ₃ OH | - 0.07716 | - 0.00669 |
| SO ₄ ²⁻ | H ₂ O | 0.02278 | 0.00271 | Br ⁻ | CH ₃ OH | - 0.00944 | - 0.06080 |
| Br ⁻ | H ₂ O | - 0.00247 | - 0.00008 | I ⁻ | CH ₃ OH | - 0.02090 | - 0.14894 |

1

| | | | | | | | |
|---------------------------|------------------------|----------|-----------|---------------------------|------------------------|---------|-----------|
| NO_2^- | H_2O | 0.00549 | - 0.00565 | F^- | CH_3OH | 0.07436 | - 0.04388 |
| I^- | H_2O | -0.00537 | 0.00018 | CH_3COO^- | CH_3OH | 0.00046 | 0.01249 |
| F^- | H_2O | 0.00652 | 0.00132 | | | | |
| CH_3COO^- | H_2O | 0.01918 | 0.00230 | | | | |
| Na^+ | CH_2CO | -0.21019 | 0.94813 | | | | |
| K^+ | CH_2CO | -0.44195 | 1.10287 | | | | |
| Cl^- | CH_2CO | 0.54064 | -0.62981 | | | | |
| Br^- | CH_2CO | 0.48898 | -0.96778 | | | | |
| I^- | CH_2CO | 0.08245 | 0.03292 | | | | |
| CH_3COO^- | CH_2CO | 0.26560 | -0.93032 | | | | |

2

3

1

Table A2: Mod. LIFAC Binary cation-anion MR interaction parameters

2

| Cation | Anion | $b_{c,a}^{(1)}$ | $b_{c,a}^{(2)}$ |
|------------------|----------------------------------|-----------------|-----------------|
| Na ⁺ | F ⁻ | -0.00694 | -0.08166 |
| Na ⁺ | I ⁻ | 0.27922 | -0.13430 |
| Na ⁺ | NO ₃ ⁻ | 0.04425 | -0.41980 |
| Na ⁺ | CH ₃ COO ⁻ | 0.25018 | 0.31363 |
| K ⁺ | F ⁻ | 0.18434 | -0.28912 |
| K ⁺ | I ⁻ | 0.12860 | 0.02379 |
| K ⁺ | NO ₃ ⁻ | -0.06095 | -0.67019 |
| K ⁺ | CH ₃ COO ⁻ | 0.27327 | 0.45129 |
| Mg ⁺ | Cl ⁻ | 0.45150 | 1.19298 |
| Mg ⁺ | Br ⁻ | 0.59615 | 1.37619 |
| Mg ⁺ | I ⁻ | 0.76336 | 1.58654 |
| Mg ⁺ | NO ₃ ⁻ | 0.28427 | 1.72405 |
| Mg ⁺ | SO ₄ ²⁻ | 0.53597 | 1.03876 |
| Ca ⁺ | Br ⁻ | 0.60948 | 0.30140 |
| Ca ⁺ | I ⁻ | 0.59261 | 1.46632 |
| Ca ⁺ | SO ₄ ²⁻ | -15.8421 | -0.00212 |
| Cu ²⁺ | Cl ⁻ | 0.21233 | 0.11695 |

| | | | |
|------------------|--------------------|---------|----------|
| Cu^{2+} | NO_3^- | 0.45706 | -0.41585 |
| Cu^{2+} | SO_4^{2-} | 1.24148 | -5.86466 |
| Zn^{2+} | Cl^- | 0.04463 | 0.43088 |

1

2

3

1

Table A3: AIOMFAC Binary cation \leftrightarrow anion MR interaction parameters.

2

| Cation | Anion | $b_{c,a}^{(1)}$ | $b_{c,a}^{(2)}$ | $b_{c,a}^{(3)}$ | $c_{c,a}^{(1)}$ | $c_{c,a}^{(2)}$ |
|-----------------|-------------------------------|-------------------------|-------------------------|--|--------------------------------------|--|
| | | [kg mol ⁻¹] | [kg mol ⁻¹] | [kg ^{1/2} mol ^{-1/2}] | [kg ² mol ⁻²] | [kg ^{1/2} mol ^{-1/2}] |
| H ⁺ | Cl ⁻ | 0.182003 | 0.243340 | 0.8 | 0.033319 | 0.504672 |
| H ⁺ | Br ⁻ | 0.120325 | 0.444859 | 0.8 | 0.080767 | 0.596776 |
| H ⁺ | NO ₃ ⁻ | 0.210638 | 0.122694 | 0.8 | -0.101736 | 1.676420 |
| H ⁺ | SO ₄ ²⁻ | 0.097108 | -0.004307 | 1.0 | 0.140598 | 0.632246 |
| H ⁺ | HSO ₄ ⁻ | 0.313812 | -4.895466 | 1.0 | -0.358419 | 0.807667 |
| Li ⁺ | Cl ⁻ | 0.106555 | 0.206370 | 0.8 | 0.053239 | 0.535548 |
| Li ⁺ | Br ⁻ | 0.106384 | 0.316480 | 0.8 | 0.057602 | 0.464658 |
| Li ⁺ | NO ₃ ⁻ | 0.076313 | 0.300550 | 0.8 | 0.046701 | 0.664928 |
| Li ⁺ | SO ₄ ²⁻ | 0.114470 | 0.035401 | 0.8 | -0.263258 | 1.316967 |
| Na ⁺ | Cl ⁻ | 0.053741 | 0.079771 | 0.8 | 0.024553 | 0.562981 |
| Na ⁺ | Br ⁻ | 0.180807 | 0.273114 | 0.8 | -0.506578 | 2.209050 |
| Na ⁺ | NO ₃ ⁻ | 0.001164 | -0.102546 | 0.410453 | 0.002535 | 0.512657 |
| Na ⁺ | SO ₄ ²⁻ | 0.001891 | -0.424184 | 0.8 | -0.223851 | 1.053620 |
| Na ⁺ | HSO ₄ ⁻ | 0.021990 | 0.001863 | 0.8 | 0.019921 | 0.619816 |

1

| | | | | | | |
|------------------------------|-------------------------------|-----------|-----------|----------|-----------|----------|
| K ⁺ | Cl ⁻ | 0.016561 | -0.002752 | 0.8 | 0.020833 | 0.670530 |
| K ⁺ | Br ⁻ | 0.033688 | 0.060882 | 0.8 | 0.015293 | 0.565063 |
| K ⁺ | NO ₃ ⁻ | 0.000025 | -0.413172 | 0.357227 | -0.000455 | 0.342244 |
| K ⁺ | SO ₄ ²⁻ | 0.004079 | -0.869936 | 0.8 | -0.092240 | 0.918743 |
| NH ₄ ⁺ | Cl ⁻ | 0.001520 | 0.049074 | 0.116801 | 0.011112 | 0.653256 |
| NH ₄ ⁺ | Br ⁻ | 0.002498 | 0.081512 | 0.143621 | 0.013795 | 0.728984 |
| NH ₄ ⁺ | NO ₃ ⁻ | -0.000057 | -0.171746 | 0.260000 | 0.005510 | 0.529762 |
| NH ₄ ⁺ | SO ₄ ²⁻ | 0.000373 | -0.906075 | 0.545109 | -0.000379 | 0.354206 |
| NH ₄ ⁺ | HSO ₄ ⁻ | 0.009054 | 0.214405 | 0.228956 | 0.017298 | 0.820465 |
| Mg ²⁺ | Cl ⁻ | 0.195909 | 0.332387 | 0.8 | 0.072063 | 0.397920 |
| Mg ²⁺ | NO ₃ ⁻ | 0.430671 | 0.767242 | 0.8 | -0.511836 | 1.440940 |
| Mg ²⁺ | SO ₄ ²⁻ | 0.122364 | -3.425876 | 0.8 | -0.738561 | 0.864380 |
| Ca ²⁺ | Cl ⁻ | 0.104920 | 0.866923 | 0.8 | 0.072063 | 0.365747 |
| Ca ²⁺ | NO ₃ ⁻ | 0.163282 | 0.203681 | 0.8 | -0.075452 | 1.210906 |

2

3

1

Table A4: UNIFAC interaction parameter (E-AIM). Values from Peng et al. (2001) are presented in red.

2

| Organics | CH _n | OH | CH ₃ OH | H ₂ O | CH ₂ CO | CHO | CCOO | HCOO | CH ₂ O | COOH |
|--------------------|-----------------|---------|--------------------|------------------|--------------------|---------|--------|---------|-------------------|--------|
| CH _n | 0.0 | 986.5 | 697.2 | 1318.0 | 476.4 | 677.0 | 232.1 | 507.00 | 251.5 | 663.5 |
| OH | 156.4 | 0.0 | -137.1 | 276.4 | 84 | -203.60 | 101.1 | 267.80 | 28.06 | 224.39 |
| CH ₃ OH | 16.51 | 249.1 | 0.0 | -181.0 | 23.39 | 306.4 | -10.72 | 179.70 | -128.60 | -202 |
| H ₂ O | -89.71 | -153.0 | 289.6 | 0.0 | -195.4 | -116.0 | 72.870 | 233.87 | 540.5 | -69.29 |
| CH ₂ CO | 26.76 | 164.5 | 108.7 | 472.5 | 0.0 | -37.36 | -213.7 | -190.40 | -103.60 | 669.4 |
| CHO | 505.7 | 529.00 | -340.2 | 480.80 | 128.0 | 0.0 | -110.3 | 766.00 | 304.1 | 497.5 |
| CCOO | 114.8 | 245.40 | 249.63 | 200.0 | 372.2 | 185.10 | 0.0 | -241.80 | -235.7 | 660.2 |
| HCOO | 329.30 | 139.40 | 227.80 | 124.63 | 385.40 | -236.50 | 1167.0 | 0.0 | -234.00 | -268.1 |
| CH ₂ O | 83.36 | 237.7 | 238.40 | -314.7 | 191.10 | -7.838 | 461.3 | 457.30 | 0.0 | 664.00 |
| COOH | 315.3 | -103.03 | 339.80 | -145.88 | -297.8 | -165.50 | -256.3 | 193.90 | -338.5 | 0.0 |

3

4

5

1

Table A5: UNIFAC Relative Vander Waals group volume (R_k) and surface area (Q_k) parameters for solvent groups.

2

| No | Family Name | Main Group | Subgroup | R_t | Q_t |
|----|-----------------|---------------------|-----------|--------|-------|
| 1 | Alkane | CH_n (n= 0,1,2,3) | CH3 | 0.9011 | 0.848 |
| | | | CH2 | 0.6744 | 0.540 |
| | | | CH | 0.4469 | 0.228 |
| | | | C | 0.2195 | 0.00 |
| 2 | Alcohol | OH | OH | 1.0000 | 1.20 |
| 3 | Water | H_2O | H_2O | 0.9200 | 1.400 |
| 4 | Methanol | CH_3OH | CH_3OH | 1.4311 | 1.432 |
| 5 | Carbonyl | CH_2CO | CH_3CO | 1.6724 | 1.488 |
| | | | CH_2CO | 1.4457 | 1.180 |
| 6 | Aldehyde | CHO | CHO | 0.9980 | 0.948 |
| 7 | Acetate | CCOO | CH_3COO | 1.9031 | 1.728 |
| | | | CH_2COO | 1.6764 | 1.420 |
| 8 | Formate | HCOO | HCOO | 1.2420 | 1.188 |
| 9 | Ether | CH_2O | CH_3O | 1.1450 | 1.088 |
| | | | CH_2O | 0.9183 | 0.780 |
| | | | CH-O | 0.6908 | 0.468 |
| 10 | Carboxylic acid | COOH | COOH | 1.3013 | 1.224 |
| | | | HCOOH | 1.5280 | 1.532 |

3

4

1 Table A6: Relative van der Waals subgroup volume (R_t^H) and surface area (Q_t^H) parameters for cations and anions considering dynamic
 2 hydration. Values from AIOMFAC and mod. LIFAC are presented in black and red, respectively.

3

| Ion | ADHN ^{a,b} | R_t | Q_t | R_t^H ^c | Q_t^H ^c | Reference |
|-------------------------------|---------------------|-------|-------|----------------------|----------------------|---------------------|
| H ⁺ | 1.93 | 0.0 | 0.0 | 1.78 | 2.70 | Zuend et al. (2008) |
| Na ⁺ | 0.22 | 0.18 | 0.18 | 0.38 | 0.62 | Zuend et al. (2008) |
| K ⁺ | 0.00 | 0.44 | 0.58 | 0.440 | 0.58 | Zuend et al. (2008) |
| NH ₄ ⁺ | 0.00 | 0.69 | 0.78 | 0.69 | 0.78 | Zuend et al. (2008) |
| Mg ²⁺ | 5.85 | 0.06 | 0.16 | 5.44 | 8.35 | Zuend et al. (2008) |
| Ca ²⁺ | 2.10 | 0.31 | 0.46 | 2.24 | 3.40 | Zuend et al. (2008) |
| Fe ²⁺ | 0.00 | 0.90 | 0.84 | 0.901 | 0.84 | ^d |
| Cu ²⁺ | 0.00 | 0.13 | 0.26 | 0.13 | 0.26 | Kiepe et al. (2006) |
| Mn ²⁺ | 0.00 | 0.90 | 0.84 | 0.901 | 0.84 | ^d |
| Zn ²⁺ | 2.18 | 0.12 | 0.24 | 2.12 | 3.29 | Kiepe et al (2006) |
| Cl ⁻ | 0.00 | 0.99 | 0.99 | 0.99 | 0.99 | Zuend et al. (2008) |
| Br ⁻ | 0.00 | 1.25 | 1.16 | 1.25 | 1.16 | Zuend et al. (2008) |
| NO ₃ ⁻ | 0.00 | 0.95 | 0.97 | 0.95 | 0.97 | Zuend et al. (2008) |
| HSO ₄ ⁻ | 0.00 | 1.65 | 1.40 | 1.65 | 1.40 | Zuend et al. (2008) |
| SO ₄ ²⁻ | 1.83 | 1.66 | 1.40 | 3.34 | 3.96 | Zuend et al. (2008) |
| OH ⁻ | 2.80 | 1.16 | 1.27 | 3.74 | 5.196 | Kiepe et al. (2006) |

| | | | | | | |
|---------------------------------------|------|-------|------|-------|--------|---------------------|
| CO_3^{2-} | 0.00 | 2.06 | 2.25 | 2.06 | 2.26 | Kiepe et al. (2006) |
| NO_2^- | 0.00 | 1.52 | 1.68 | 1.52 | 1.6 | Kiepe et al. (2006) |
| I^- | 0.00 | 1.55 | 1.34 | 1.55 | 1.34 | Kiepe et al. (2006) |
| F^- | 5.02 | 0.29 | 0.44 | 4.92 | 7.45 | Kiepe et al. (2006) |
| HCOO^- | 0.00 | 0.901 | 0.84 | 0.901 | 0.84 | ^d |
| CH_3COO^- | 0.00 | 1.74 | 1.04 | 1.74 | 1.0437 | Kiepe et al. (2006) |
| $\text{HOOCCH}_2\text{COO}^-$ | 0.00 | 0.901 | 0.84 | 0.901 | 0.84 | ^d |
| $\text{HOCC}_2\text{H}_4\text{COO}^-$ | 0.00 | 0.901 | 0.84 | 0.901 | 0.84 | ^d |
| HCO_3^- | 0.00 | 0.901 | 0.84 | 0.901 | 0.84 | ^d |
| CHOCOO^- | 0.00 | 0.901 | 0.84 | 0.901 | 0.84 | ^d |

¹ The apparent dynamic hydration numbers (ADHN) at 303.15 K and 0.1 M take from Kiriukhin and Collins (2002).

^b Values of ADHN = 0 are assigned to the ions for which the data is unavailable.

^c calculated using Eq. (34) and (35), respectively.

^d ADHN data is not available

1

2

3

1 Appendix B: List of symbols, indices and acronyms

2 Table B1. List and description of symbols and indices.

| Symbol/Index | Description |
|--|---|
| a_i | Activity of species i |
| a_A | Activity of compound A |
| a_i^k | Activity of species i in the k^{th} particle/cloud droplet class |
| a_w | Water activity |
| a_w^k | Water activity in the k^{th} particle/cloud droplet class |
| $A_{(aq)}$ | Compound A in the aqueous phase |
| $A_{(g)}$ | Compound A in the gas phase |
| A | Debye-Hückel parameter |
| b | Debye-Hückel parameter |
| $B_{c,a}(I)$ | Ionic strength dependent binary interaction coefficient between cations and anions |
| $b_{k,i}^{(1)}, b_{k,i}^{(2)}, b_{c,a}^{(1)}, b_{c,a}^{(2)}, c_{c,a}^{(1)}, c_{c,a}^{(2)}$ | Fitted parameters (AIOMFAC) |
| $B_{k,i}(I)$ | Ionic strength dependent binary interaction coefficient between solvent main groups and ions |
| c^* | Specific cation |
| $C_{c,a}(I)$ | Interaction coefficient between cation \leftrightarrow anion pairs with respect to the total charge concentration |
| c^G | Vector of the concentrations of the gas phase species |
| c_i | Mass concentration of an aqueous phase species i |
| $c_{i,k}^s$ | Saturation vapor mole concentration |
| c_i^G | i^{*th} gas phase chemical species |
| \mathbf{c}^k | Vector of all concentrations |
| c_i^k | i^{th} aqueous phase chemical species in the k^{th} particle/cloud droplet class |
| c_{sol} | Solute concentration |
| c_{sol}^k | Solute concentration in the k^{th} particle class |
| D_i^G | Gas diffusion coefficient |
| $F(c_l^1, \dots, c_l^M)$ | Mass transfer between different droplet classes by microphysical processes |
| G_{LR}^{ex} | Long-range (LR) electrostatic interactions contributing to excess Gibbs free energy |
| G_{MR}^{ex} | Middle-range (MR) electrostatic interactions contributing to excess Gibbs free energy |
| G_{SR}^{ex} | Short-range (SR) electrostatic interactions contributing to excess Gibbs free energy |
| $G^{ex}(p, T, n_j)$ | Excess Gibbs energy |

| Symbol/Index | Description |
|-------------------|--|
| H_i | Dimensionless Henry's law constant of species i |
| i, i^* | Species index |
| I | Identity matrix |
| I | Ionic strength |
| j | Species index |
| J | Approximation of the Jacobian |
| $k = 1, \dots, M$ | Particle/cloud droplet class index |
| k_i^{ki} | Mass transfer coefficient of species i into the k^{th} particle/cloud droplet class |
| K_{eq} | Equilibrium constant |
| K_i^H | Henry's law constant of species i |
| L | Liquid water content |
| L_k | Liquid water content of the k^{th} droplet class inside the box volume |
| m_A | Molality of compound A |
| M_c | Molar mass of carbon |
| m_i | Molality of an aqueous phase species i |
| m_i^k | Molality of dissolved gas phase species i in particle class k |
| m_j | Molality of the j^{th} species |
| $mol_{sol_i}^k$ | Moles of soluble material of the i^{th} species in the k^{th} particle/droplet class |
| M_{sol} | Mean molar mass of solute |
| M_s | Molar mass of solvent s |
| mol_w^k | Molar water fraction |
| N_A | Number of aqueous phase species |
| n_a | Moles of anions |
| N_t^{ADH} | Dynamic hydration numbers |
| $n_c, n_{c'}$ | Moles of cations |
| n_{cb} | Number of carbon atoms |
| N_G | Number of gas phase species |
| n_j | Number of moles of component j |
| P | Total pressure |
| $P_{i,k}^s$ | Saturation vapor pressure of gas phase species i over a particle in size bin k |
| P_w | Equilibrium partial pressure of water over the solution droplet |
| P_w^o | Equilibrium water vapor pressure over a flat surface of pure water |
| $Q_{c,c',a}(I)$ | Ternary interaction coefficient involving two different cations |
| q_i / r_i | Surface area / volume of component i |

| Symbol/Index | Description |
|----------------------------------|---|
| r_A | Reaction rate |
| $r_{drop} (m)$ | Mean wet droplet radius |
| r_k | Droplet radius of the k^{th} particle/cloud droplet class |
| R | Universal gas constant |
| $R_{c,c'}(I)$ | Binary interaction coefficient involving two different cations |
| RH | Ambient relative humidity |
| R_l^A | Aqueous phase chemical reaction terms of species l (chemical production and degradation fluxes) |
| R_l^G | Gas phase chemical reaction terms of species l^* (chemical production and degradation fluxes) |
| R_i / Q_i | Relative van der Waals subgroup volume/surface area parameters |
| R_i^H / Q_i^H | Hydrated group volume and surface area parameters |
| R_w / Q_w | R_i / Q_i values of the water molecule |
| $T (K)$ | Temperature |
| x_w | Mole fraction of water |
| x_i | Mole fraction of component i |
| z_i | Number of elementary charges of ion i |
| $\{a_i\}$ | Thermodynamic activity of species i |
| $\{A\}$ etc. | Individual thermodynamic activities |
| $\{A_{(aq)}\} = m_A \gamma_A$ | Activity of an un-dissociated compound |
| $\{A_{(g)}\}$ | Activity of a gas over a particle surface |
| $\{A_{(s)}\} = m_s$ | Activity of a solid |
| $\{A^+\} = m_{A^+} \gamma_{A^+}$ | Activity of an ion in solution |
| $[C^k]$ | Concentration of WSOC (Water Soluble Organic Carbon) in particle class k |
| $\{H_2O_{(aq)}\} = a_w$ | Activity of liquid water in a particle |
| α_i | Mass accommodation coefficient of the i^{th} species |
| β | Parameter of the integration method |
| γ_A | Activity coefficient of compound A |
| γ_i | Molality based activity coefficient of species i |
| γ_w | Molality based water activity coefficient |
| γ_j^k | Activity coefficient of the j^{th} species in the k^{th} particle/droplet class |
| γ_{\pm} | Mean activity coefficient |
| γ_+ / γ_- | Activity coefficients of a cation and anion |
| ϵ_w | Static permittivity |

| Symbol/Index | Description |
|---|---|
| κ_l | Prefactor of the Henry term (solubility index) |
| $\lambda_i (= \pm 1)$ | Factor +1 for products and -1 for reactants |
| μ | Time dependent entrainment/detrainment rate |
| $\mu_i^{(m)}(p, T, n_j) / \mu_i^{(x)}(p, T, n_j)$ | Chemical potentials |
| v_i | Molecular speed of gas phase species i |
| v_w | Partial molar volume of water |
| ρ_w | Density |
| σ_w | Surface tension of pure water |
| $\sigma_{w,s}$ | Droplet solution surface tension |
| $\ln \gamma_j^{SR}$ | Short-range activity coefficient γ_j of a molecular component j (can be solute or solvent) |
| $\ln \gamma_i^{SR,(x),\infty}$ | Unsymmetrical normalized activity coefficient |

1

2

3 Table B2. List and description of acronyms.

| Acronym | Description |
|--------------|--|
| ADCHAM | Aerosol Dynamics, gas- and particle-phase chemistry model for laboratory CHAMber studies |
| ADDEM | Aerosol Diameter Dependent Equilibrium Model |
| AIM | Aerosol Inorganic Model |
| GFEMN | Gibbs free energy minimization model |
| AIOMFAC | Aerosol Inorganic-Organic Mixtures Functional groups Activity Coefficients |
| BDF | Backward differential formula |
| CAPRAM | Chemical Aqueous Phase RADical Mechanism |
| CSB | Clegg-Seinfeld-Brimblecombe model |
| E-AIM | Extended Aerosol Inorganic Model |
| EQSAM3 | 3rd Equilibrium Simplified Aerosol Model (EQSAM3) |
| EQUISOLV II | EQUilibrium SOLVer version 2 |
| ISORROPIA | Thermodynamic equilibrium aerosol model (= "equilibrium" in Greek) |
| ISORROPIA II | Thermodynamic equilibrium aerosol model version 2 |
| LR | Long-range |
| MADM | Multicomponent Aerosol Dynamics Model |
| MARS-A | Model for an Aerosol Reacting System – version A |

| Acronym | Description |
|------------|--|
| MESA | Multicomponent Equilibrium Solver for Aerosols |
| mod. LIFAC | Modified Liquid Functional Activity Coefficient Model |
| MOSAIC | MOdel for Simulating Aerosol Interactions and Chemistry |
| MR | Middle-range |
| ODE | Ordinary differential equation |
| SPACCIM | Spectral Aerosol Cloud Chemistry Interaction Model |
| SpactMod | SPACCIM activity coefficient module |
| SR | Short-range |
| TMIs | Transition Metal Ions |
| UHAERO | Inorganic atmospheric aerosol phase equilibrium model (UHAERO) |
| UNIFAC | UNIversal Functional-group Activity Coefficients |
| WSOC | Water Soluble Organic Carbon |

1

2

3

1

2 **Acknowledgement**

3 The authors would like to thank Claudia Marcolli and Thomas Peter (ETH Zurich) for the
4 performed water activity measurements of the aqueous test solutions. Furthermore, we would
5 like to thank Andreas Zünd (Mc Gill University, Montreal) for providing a set of additional
6 interaction parameters of AIOMFAC.

7

8 **References**

9

- 10 Achard, C., Dussap, C. G., and Gros, J. B.: Representation of vapour-liquid equilibria in
11 water-alcohol-electrolyte mixtures with a modified UNIFAC-group-contribution method,
12 *Fluid Phase Equilibr.*, 98, 71-89, 1994.
- 13 Amundson, N. R., Caboussat, A., He, J. W., Martynenko, A. V., Savarin, V. B., Seinfeld, J.
14 H., and Yoo, K. Y.: A new inorganic atmospheric aerosol phase equilibrium model
15 (UHAERO), *Atmos. Chem. Phys.*, 6, 975-992, 2006.
- 16 Amundson, N. R., Caboussat, A., He, J. W., Martynenko, A. V., Landry, C., Tong, C., and
17 Seinfeld, J. H.: A new atmospheric aerosol phase equilibrium model (UHAERO): organic
18 systems, *Atmos. Chem. Phys.*, 7, 4675-4698, 10.5194/acp-7-4675-2007, 2007.
- 19 Ansari, A. S., and Pandis, S. N.: Prediction of multicomponent inorganic atmospheric aerosol
20 behavior, *Atmos. Environ.*, 33, 745-757, 1999a.
- 21 Ansari, A. S., and Pandis, S. N.: An analysis of four models predicting the partitioning of
22 semivolatile inorganic aerosol components, *Aerosol Sci Tech*, 31, 129-153, Doi
23 10.1080/027868299304200, 1999b.
- 24 Antypov, D., and Holm, C.: Osmotic coefficient calculations for dilute solutions of short stiff-
25 chain polyelectrolytes, *Macromolecules*, 40, 731-738, 2007.
- 26 Binkowski, F. S., and Roselle, S. J.: Models-3 Community Multiscale Air Quality (CMAQ)
27 model aerosol component 1. Model description, *J. Geophys. Res. Atmos.*, 108, 2003.
- 28 Bräuer, P., Tilgner, A., Wolke, R., and Herrmann, H.: Mechanism development and
29 modelling of tropospheric multiphase halogen chemistry: The CAPRAM Halogen Module 2.0
30 (HM2), *J. Atmos. Chem.*, 70, 19-52, 10.1007/S10874-013-9249-6, 2013.
- 31 Chang, E. I., and Pankow, J. F.: Prediction of activity coefficients in liquid aerosol particles
32 containing organic compounds, dissolved inorganic salts, and water - Part 2: Consideration of
33 phase separation effects by an X-UNIFAC model, *Atmos. Environ.*, 40, 6422-6436, 2006.
- 34 Clegg, S. L., Brimblecombe, P., and Wexler, A. S.: A thermodynamic model of the system H^+
35 - NH_4^+ - SO_4^{2-} - NO_3^- - H_2O at 298.15 K, *J. Phys. Chem. A*, 102, 2155-2171, 1998a.
- 36 Clegg, S. L., Brimblecombe, P., and Wexler, A. S.: Thermodynamic Model of the System H^+
37 - NH_4^+ - SO_4^{2-} - NO_3^- - H_2O at Tropospheric Temperatures, *J. Phys. Chem. A*, 102, 2137-
38 2154, 1998b.

- 1 Clegg, S. L., Seinfeld, J. H., and Brimblecombe, P.: Thermodynamic modelling of aqueous
2 aerosols containing electrolytes and dissolved organic compounds, *J. Aerosol. Sci.*, 32, 713-
3 738, 2001.
- 4 Clegg, S. L., Kleeman, M. J., Griffin, R. J., and Seinfeld, J. H.: Effects of uncertainties in the
5 thermodynamic properties of aerosol components in an air quality model - Part 1: Treatment
6 of inorganic electrolytes and organic compounds in the condensed phase, *Atmos. Chem.*
7 *Phys.*, 8, 1057-1085, 2008.
- 8 Debye, P., and Hückel, E.: Zur Theorie der Elektrolyte, *Physikalische Zeitschrift*, 24, 185-
9 206, 1923.
- 10 Deguillaume, L., Tilgner, A., Schrodner, R., Wolke, R., Chaumerliac, N., and Herrmann, H.:
11 Towards an operational aqueous phase chemistry mechanism for regional chemistry-transport
12 models: CAPRAM-RED and its application to the COSMO-MUSCAT model, *J. Atmos.*
13 *Chem.*, 64, 1-35, 10.1007/S10874-010-9168-8, 2010.
- 14 Demaret, J. P., and Gueron, M.: Composite cylinder models of DNA - Application of the
15 electrostatics of the B-Z transition, *Biophys. J.*, 65, 1700-1713, 1993.
- 16 Erdakos, G. B., Chang, E. I., Pankow, J. F., and Seinfeld, J. H.: Prediction of activity
17 coefficients in liquid aerosol particles containing organic compounds, dissolved inorganic
18 salts, and water-Part 3: Organic compounds, water, and ionic constituents by consideration of
19 short-, mid-, and long-range effects using X-UNIFAC.3, *Atmos. Environ.*, 40, 6437-6452,
20 2006.
- 21 Ervens, B., George, C., Williams, J. E., Buxton, G. V., Salmon, G. A., Bydder, M.,
22 Wilkinson, F., Dentener, F., Mirabel, P., Wolke, R., and Herrmann, H.: CAPRAM 2.4
23 (MODAC mechanism): An extended and condensed tropospheric aqueous phase mechanism
24 and its application, *J. Geophys. Res. Atmos.*, 108, 10.1029/2002jd002202, 2003.
- 25 Ervens, B., Feingold, G., Clegg, S. L., and Kreidenweis, S. M.: A modeling study of aqueous
26 production of dicarboxylic acids: 2. Implications for cloud microphysics, *J. Geophys. Res.*
27 *Atmos.*, 109, 2004.
- 28 Ervens, B., Turpin, B. J., and Weber, R. J.: Secondary organic aerosol formation in cloud
29 droplets and aqueous particles (aqSOA): a review of laboratory, field and model studies,
30 *Atmos. Chem. Phys.*, 11, 11069-11102, 10.5194/Acp-11-11069-2011, 2011.
- 31 Facchini, M., Mircea, M., Fuzzi, S., and Charlson, R.: Cloud albedo enhancement by surface-
32 active organic solutes in growing droplets, *Nature*, 401, 257-259, 1999.
- 33 Facchini, M. C., Decesari, S., Mircea, M., Fuzzi, S., and Loglio, G.: Surface tension of
34 atmospheric wet aerosol and cloud/fog droplets in relation to their organic carbon content and
35 chemical composition, *Atmos Environ*, 34, 4853-4857, Doi 10.1016/S1352-2310(00)00237-5,
36 2000.
- 37 Fast, J. D., Gustafson, W. I., Easter, R. C., Zaveri, R. A., Barnard, J. C., Chapman, E. G.,
38 Grell, G. A., and Peckham, S. E.: Evolution of ozone, particulates, and aerosol direct radiative
39 forcing in the vicinity of Houston using a fully coupled meteorology-chemistry-aerosol
40 model, *J. Geophys. Res. Atmos.*, 111, 2006.
- 41 Fountoukis, C., and Nenes, A.: ISORROPIA II: a computationally efficient thermodynamic
42 equilibrium model for K^+ - Ca^{2+} - Mg^{2+} - NH_4^+ - Na^+ - SO_4^{2-} - NO_3^- - Cl^- - H_2O aerosols,
43 *Atmos. Chem. Phys.*, 7, 4639-4659, 2007.

- 1 Fredenslund, A., Jones, R. L., and Prausnitz, J. M.: Group-contribution estimation of activity
2 coefficients in non-ideal liquid mixtures, *AIChE J.*, 21, 1086-1098, 1975.
- 3 Ganbavale, G., Zuend, A., Marcolli, C., and Peter, T.: Improved AIOMFAC model
4 parameterisation of the temperature dependence of activity coefficients for aqueous organic
5 mixtures, *Atmos Chem Phys*, 15, 447-493, 10.5194/acp-15-447-2015, 2015.
- 6 Gilardoni, S., Liu, S., Takahama, S., Russell, L. M., Allan, J. D., Steinbrecher, R., Jimenez, J.
7 L., De Carlo, P. F., Dunlea, E. J., and Baumgardner, D.: Characterization of organic ambient
8 aerosol during MIRAGE 2006 on three platforms, *Atmos. Chem. Phys.*, 9, 5417-5432, 2009.
- 9 Guo, J., Tilgner, A., Yeung, C., Wang, Z., Louie, P. K. K., Luk, C. W. Y., Xu, Z., Yuan, C.,
10 Gao, Y., Poon, S., Herrmann, H., Lee, S., Lam, K. S., and Wang, T.: Atmospheric Peroxides
11 in a Polluted Subtropical Environment: Seasonal Variation, Sources and Sinks, and
12 Importance of Heterogeneous Processes, *Environ. Sci. & Technol.*, 48, 1443-1450,
13 10.1021/Es403229x, 2014.
- 14 Hairer, E., Nørsett, S. P., and Wanner, G.: Solving Ordinary Differential Equations: Stiff and
15 differential-algebraic problems, Springer, 1993.
- 16 Hallquist, M., Wenger, J. C., Baltensperger, U., Rudich, Y., Simpson, D., Claeys, M.,
17 Dommen, J., Donahue, N. M., George, C., Goldstein, A. H., Hamilton, J. F., Herrmann, H.,
18 Hoffmann, T., Iinuma, Y., Jang, M., Jenkin, M. E., Jimenez, J. L., Kiendler-Scharr, A.,
19 Maenhaut, W., McFiggans, G., Mentel, T. F., Monod, A., Prevot, A. S. H., Seinfeld, J. H.,
20 Surratt, J. D., Szmigielski, R., and Wildt, J.: The formation, properties and impact of
21 secondary organic aerosol: Current and emerging issues, *Atmos. Chem. Phys.*, 9, 5155-5236,
22 2009.
- 23 Hamer, W. J., and Wu, Y. C.: Osmotic Coefficients and Mean Activity Coefficients of Uni-
24 Univalent Electrolytes in Water at 25 °C, *J. Phys. Chem. Ref. Data*, 1, 1047-1100, 1972.
- 25 Hansen, H. K., Rasmussen, P., Fredenslund, A., Schiller, M., and Gmehling, J.: Vapor-liquid
26 equilibria by UNIFAC group contribution. 5. Revision and extension, *Ind. Eng. Chem. Res.*,
27 30, 2352-2355, 1991.
- 28 Henning, S., Rosenorn, T., D'Anna, B., Gola, A. A., Svenningsson, B., and Bilde, M.: Cloud
29 droplet activation and surface tension of mixtures of slightly soluble organics and inorganic
30 salt, *Atmos Chem Phys*, 5, 575-582, 2005.
- 31 Herrmann, H.: Kinetics of aqueous phase reactions relevant for atmospheric chemistry, *Chem.*
32 *Rev.*, 103, 4691-4716, 10.1021/Cr020658q, 2003.
- 33 Herrmann, H., Tilgner, A., Barzagli, P., Majdik, Z.-T., Gligorovski, S., Poulain, L., and
34 Monod, A.: Towards a more detailed description of tropospheric aqueous phase organic
35 chemistry: CAPRAM 3.0, *Atmos. Environ.*, 39, 4351-4363, 2005.
- 36 Herrmann, H., Schaefer, T., Tilgner, A., Styler, S. A., Weller, C., Teich, M., and Otto, T.:
37 Tropospheric Aqueous-Phase Chemistry: Kinetics, Mechanisms, and Its Coupling to a
38 Changing Gas Phase, *Chem Rev*, 115, 4259-4334, 10.1021/cr500447k, 2015.
- 39 Iliuta, M. C., Thomson, K., and Rasmussen, P.: Extended UNIQUAC model for correlation
40 and prediction of vapour-liquid-solid equilibria in aqueous salt systems containing non-
41 electrolytes. Part A. Methanol-water-salt systems, *Chem. Eng. Sci.*, 55, 2673-2686, 2000.
- 42 Jacobson, M. Z., Tabazadeh, A., and Turco, R. P.: Simulating equilibrium within aerosols and
43 nonequilibrium between gases and aerosols, *J. Geophys. Res. Atmos.*, 101(D4), 9071-9091,
44 1996.

1 Jacobson, M. Z.: Development and application of a new air pollution modeling system .Part
2 II. Aerosol module structure and design, *Atmos. Environ.*, 31, 131-144, 1997.

3 Jungwirth, P., and Tobias, D. J.: Molecular Structure of Salt Solutions: A New View of the
4 Interface with Implications for Heterogeneous Atmospheric Chemistry, *J. Phys. Chem. B*,
5 105, 10468-10472, 2001.

6 Kiepe, J., Noll, O., and Gmehling, J.: Modified LIQUAC and Modified LIFACA Further
7 Development of Electrolyte Models for the Reliable Prediction of Phase Equilibria with
8 Strong Electrolytes, *Ind. Eng. Chem. Res.*, 45, 2361-2373, 2006.

9 Kiriukhin, M. Y., and Collins, K. D.: Dynamic hydration numbers for biologically important
10 ions, *Biophys. Chem.*, 99, 155-168, 2002.

11 Knopf, D. A., Luo, B. P., Krieger, U. K., and Koop, T.: Thermodynamic dissociation constant
12 of the bisulfate ion from Raman and ion interaction modeling studies of aqueous sulfuric acid
13 at low temperatures, *J. Phys. Chem. A*, 107, 4322-4332, 2003.

14 Köhler, H.: The nucleus in and the growth of hygroscopic droplets, *Trans. Faraday Soc.*, 32,
15 1152-1161, 1936.

16 Li, J. D., Polka, H. M., and Gmehling, J.: A GE model for single and mixed solvent
17 electrolyte systems. 1. Model and results for strong electrolytes, *Fluid Phase Equilib.*, 94, 89-
18 114, 1994.

19 Liu, S., Takahama, S., Russell, L. M., Gilardoni, S., and Baumgardner, D.: Oxygenated
20 organic functional groups and their sources in single and submicron organic particles in
21 MILAGRO 2006 campaign, *Atmos. Chem. Phys.*, 9, 6849-6863, 2009.

22 Maffia, M. C., and Meirelles, A. J. A.: Water activity and pH in aqueous polycarboxylic acid
23 systems, *J Chem Eng Data*, 46, 582-587, DOI 10.1021/je0002890, 2001.

24 Mao, J., Fan, S., Jacob, D. J., and Travis, K. R.: Radical loss in the atmosphere from Cu-Fe
25 redox coupling in aerosols, *Atmos Chem Phys*, 13, 509-519, 10.5194/acp-13-509-2013, 2013.

26 Marcolli, C., and Peter, T.: Water activity in Polyol/water systems: new UNIFAC
27 parametrization, *Atmos. Chem. Phys.*, 5, 1545-1555, 2005.

28 Metzger, S., Dentener, F., Pandis, S., and Lelieveld, J.: Gas/aerosol partitioning: 1. A
29 computationally efficient model, *J Geophys Res-Atmos*, 107, Artn 4312
30 10.1029/2001jd001102, 2002.

31 Metzger, S., Mihalopoulos, N., and Lelieveld, J.: Importance of mineral cations and organics
32 in gas-aerosol partitioning of reactive nitrogen compounds: case study based on MINOS
33 results, *Atmos. Chem. Phys.*, 6, 2549-2567, 2006.

34 Metzger, S., and Lelieveld, J.: Reformulating atmospheric aerosol thermodynamics and
35 hygroscopic growth into fog, haze and clouds, *Atmos. Chem. Phys.*, 7, 3163-3193, 2007.

36 Ming, Y., and Russell, L. M.: Thermodynamic equilibrium of organic-electrolyte mixtures in
37 aerosol particles, *AIChE Journal*, 48, 1331-1348, 2002.

38 Mircea, M., Facchini, M. C., Decesari, S., Fuzzi, S., and Charlson, R. J.: The influence of the
39 organic aerosol component on CCN supersaturation spectra for different aerosol types, *Tellus*
40 B, 54, 74-81, DOI 10.1034/j.1600-0889.2002.00256.x, 2002.

- 1 Mohs, A., and Gmehling, J.: A revised LIQUAC and LIFAC model (LIQUAC*/LIFAC*) for
2 the prediction of properties of electrolyte containing solutions, *Fluid Phase Equilibr*, 337,
3 311-322, 10.1016/j.fluid.2012.09.023, 2013.
- 4 Nenes, A., Pandis, S. N., and Pilinis, C.: ISORROPIA: A New Thermodynamic Equilibrium
5 Model for Multiphase Multicomponent Inorganic Aerosols, *Aquat. Geochem.*, 4, 123-152,
6 1998.
- 7 Nenes, A., Charlson, R. J., Facchini, M. C., Kulmala, M., Laaksonen, A., and Seinfeld, J. H.:
8 Can chemical effects on cloud droplet number rival the first indirect effect?, *Geophys Res*
9 *Lett*, 29, 10.1029/2002gl015295, 2002.
- 10 Peng, C., Chan, M. N., and Chan, C. K.: The hygroscopic properties of dicarboxylic and
11 multifunctional acids: Measurements and UNIFAC predictions, *Environ Sci Technol*, 35,
12 4495-4501, 10.1021/Es0107531, 2001.
- 13 Pilinis, C., Capaldo, K. P., Nenes, A., and Pandis, S. N.: MADM-A New Multicomponent
14 Aerosol Dynamics Model, *Aerosol Sci. Technol.*, 32, 482-502, 2000.
- 15 Pitzer, K. S.: Activity coefficients in electrolyte solutions, CRC Press, 1991.
- 16 Prausnitz, J. M., Lichtenthaler, R. N., and De Azevedo, E. G.: Molecular Thermodynamics of
17 Fluid-Phase Equilibria, Prentice-Hall Inc., Englewood Cliffs, New Jersey, USA, 2nd edn.,
18 1986.
- 19 Prisle, N. L., Dal Maso, M., and Kokkola, H.: A simple representation of surface active
20 organic aerosol in cloud droplet formation, *Atmos Chem Phys*, 11, 4073-4083, 10.5194/acp-
21 11-4073-2011, 2011.
- 22 Prisle, N. L., Ottosson, N., Ohrwall, G., Soderstrom, J., Dal Maso, M., and Bjorneholm, O.:
23 Surface/bulk partitioning and acid/base speciation of aqueous decanoate: direct observations
24 and atmospheric implications, *Atmos Chem Phys*, 12, 12227-12242, 10.5194/acp-12-12227-
25 2012, 2012.
- 26 Pruppacher, H. R., and Klett, J. D.: Microphysics of Clouds and Precipitation, Dordrecht, The
27 Netherlands, Kluwer Academic Publishers, 1997.
- 28 Raatikainen, T., and Laaksonen, A.: Application of several activity coefficient models to
29 water-organic-electrolyte aerosols of atmospheric interest, *Atmos. Chem. Phys.*, 5, 2475-
30 2495, 10.5194/acp-5-2475-2005, 2005.
- 31 Raatikainen, T., and Laaksonen, A.: A simplified treatment of surfactant effects on cloud drop
32 activation, *Geosci Model Dev*, 4, 107-116, 10.5194/gmd-4-107-2011, 2011.
- 33 Ravishankara, A. R.: Heterogeneous and Multiphase Chemistry in the Troposphere, *Science*,
34 276, 1058-1065, 1997.
- 35 Roldin, P., Eriksson, A. C., Nordin, E. Z., Hermansson, E., Mogensen, D., Rusanen, A., Boy,
36 M., Swietlicki, E., Svenningsson, B., Zelenyuk, A., and Pagels, J.: Modelling non-equilibrium
37 secondary organic aerosol formation and evaporation with the aerosol dynamics, gas- and
38 particle-phase chemistry kinetic multilayer model ADCHAM, *Atmos Chem Phys*, 14, 7953-
39 7993, 10.5194/Acp-14-7953-2014, 2014.
- 40 Russell, L. M., Takahama, S., Liu, S., Hawkins, L. N., Covert, D. S., Quinn, P. K., and Bates,
41 T. S.: Oxygenated fraction and mass of organic aerosol from direct emission and atmospheric
42 processing measured on the R/V Ronald Brown during TEXAQS/GoMACCS 2006, *J.*
43 *Geophys. Res.-Atmos.*, 114, 2009.

- 1 Rusumdar, A. J., Tilgner, A., Wolke, R., and Herrmann, H.: Treatment of non-ideality in the
2 multiphase model SPACCIM- Part 2: Model studies on the multiphase chemical processing in
3 deliquesced particles, in preparation for *Atmos. Chem. Phys.*, 2015.
- 4 Sander, R.: Compilation of Henry's law constants (version 4.0) for water as solvent, *Atmos*
5 *Chem Phys*, 15, 4399-4981, 10.5194/acp-15-4399-2015, 2015.
- 6 Saxena, P., Hudischewskyj, A. B., Seigneur, C., and Seinfeld, J. H.: A comparative study of
7 equilibrium approaches to the chemical characterization of secondary aerosols, *Atmos.*
8 *Environ.*, 20, 1471-1483, 1986.
- 9 Schwartz, S. E.: Mass transport considerations pertinent to aqueous phase reactions of gases
10 in liquid water clouds, In: *Chemistry of Multiphase Atmospheric Systems*, W. Jaeschke, ed.,
11 Springer, Berlin, 415-471, 1986.
- 12 Sehili, A. M., Wolke, R., Knoth, O., Simmel, M., Tilgner, A., and Herrmann, H.: Comparison
13 of different model approaches for the simulation of multiphase processes, *Atmos. Environ.*,
14 39, 4403-4417, 2005.
- 15 Seinfeld, J. H., and Pandis, S. N.: *Atmospheric Chemistry and Physics- From Air Pollution to*
16 *Climate Change*, 2. edition, John Wiley & Sons Inc., New York, USA, 2006.
- 17 Shrivastava, M., Fast, J., Easter, R., Gustafson, W. I., Zaveri, R. A., Jimenez, J. L., Saide, P.,
18 and Hodzic, A.: Modeling organic aerosols in a megacity: comparison of simple and complex
19 representations of the volatility basis set approach, *Atmos. Chem. Phys.*, 11, 6639-6662,
20 10.5194/Acp-11-6639-2011, 2011.
- 21 Shulman, M. L., Jacobson, M. C., Carlson, R. J., Synovec, R. E., and Young, T. E.:
22 Dissolution behavior and surface tension effects of organic compounds in nucleating cloud
23 droplets, *Geophys Res Lett*, 23, 277-280, Doi 10.1029/95gl03810, 1996.
- 24 Simmel, M., and Wurzler, S.: Condensation and activation in sectional cloud microphysical
25 models, *Atmos. Environ.*, 80, 218-236, 2006.
- 26 Sorjamaa, R., Svenningsson, B., Raatikainen, T., Henning, S., Bilde, M., and Laaksonen, A.:
27 The role of surfactants in Kohler theory reconsidered, *Atmos Chem Phys*, 4, 2107-2117,
28 2004.
- 29 Sorjamaa, R., and Laaksonen, A.: The influence of surfactant properties on critical
30 supersaturations of cloud condensation nuclei, *J Aerosol Sci*, 37, 1730-1736,
31 10.1016/j.jaerosci.2006.07.004, 2006.
- 32 Svenningsson, B., Rissler, J., Swietlicki, E., Mircea, M., Bilde, M., Facchini, M. C., Decesari,
33 S., Fuzzi, S., Zhou, J., Monster, J., and Rosenorn, T.: Hygroscopic growth and critical
34 supersaturations for mixed aerosol particles of inorganic and organic compounds of
35 atmospheric relevance, *Atmos Chem Phys*, 6, 1937-1952, 2006.
- 36 Takahama, S., Schwartz, R. E., Russell, L. M., Macdonald, A. M., Sharma, S., and Leitch,
37 W. R.: Organic functional groups in aerosol particles from burning and non-burning forest
38 emissions at a high-elevation mountain site, *Atmos. Chem. Phys.*, 11, 6367-6386, 2011.
- 39 Tilgner, A., and Herrmann, H.: Radical-driven carbonyl-to-acid conversion and acid
40 degradation in tropospheric aqueous systems studied by CAPRAM, *Atmos. Environ.*, 44,
41 5415-5422, 2010.
- 42 Tilgner, A., Bräuer, P., Wolke, R., and Herrmann, H.: Modelling multiphase chemistry in
43 deliquescent aerosols and clouds using CAPRAM3.0i, *J. Atmos. Chem.*, 70, 221-256, 2013.

- 1 Tong, C., Clegg, S. L., and Seinfeld, J. H.: Comparison of activity coefficient models for
2 atmospheric aerosols containing mixtures of electrolytes, organics, and water, *Atmos.*
3 *Environ.*, 42, 5459-5482, 2008.
- 4 Topping, D.: An analytical solution to calculate bulk mole fractions for any number of
5 components in aerosol droplets after considering partitioning to a surface layer, *Geosci Model*
6 *Dev.*, 3, 635-642, 10.5194/gmd-3-635-2010, 2010.
- 7 Topping, D., Connolly, P., and McFiggans, G.: Cloud droplet number enhanced by co-
8 condensation of organic vapours, *Nat Geosci.*, 6, 443-446, 10.1038/Ngeo1809, 2013.
- 9 Topping, D. O., McFiggans, G. B., and Coe, H.: A curved multi-component aerosol
10 hygroscopicity model framework: Part 1 - Inorganic compounds, *Atmos. Chem. Phys.*, 5,
11 1205-1222, 2005a.
- 12 Topping, D. O., McFiggans, G. B., and Coe, H.: A curved multi-component aerosol
13 hygroscopicity model framework: Part 2 - Including organic compounds, *Atmos. Chem.*
14 *Phys.*, 5, 1223-1242, 2005b.
- 15 Topping, D. O., McFiggans, G. B., Kiss, G., Varga, Z., Facchini, M. C., Decesari, S., and
16 Mircea, M.: Surface tensions of multi-component mixed inorganic/organic aqueous systems
17 of atmospheric significance: measurements, model predictions and importance for cloud
18 activation predictions, *Atmos Chem Phys*, 7, 2371-2398, 2007.
- 19 Tuckermann, R., and Cammenga, H. K.: The surface tension of aqueous solutions of some
20 atmospheric water-soluble organic compounds, *Atmos Environ*, 38, 6135-6138,
21 10.1016/j.atmosenv.2004.08.005, 2004.
- 22 Wexler, A., Clegg, S., and L., S.: Atmospheric aerosol models for systems including the ions
23 H⁺, NH₄⁺, Na⁺, SO₄²⁻, NO₃⁻, Cl⁻, Br⁻, and H₂O, *J. Geophys. Res.-Atmos.*, 107, 2002.
- 24 Wexler, A. S., and Seinfeld, J. H.: The Distribution of Ammonium-Salts among a Size and
25 Composition Dispersed Aerosol, *Atmos Environ a-Gen*, 24, 1231-1246, Doi 10.1016/0960-
26 1686(90)90088-5, 1990.
- 27 Wolke, R., and Knöth, O.: Time-integration of multiphase chemistry in size-resolved cloud
28 models, *Appl. Numer. Math.*, 42, 473-487, 2002.
- 29 Wolke, R., Sehili, A. M., Simmel, M., Knöth, O., Tilgner, A., and Herrmann, H.: SPACCIM:
30 A parcel model with detailed microphysics and complex multiphase chemistry, *Atmos.*
31 *Environ.*, 39, 4375-4388, 2005.
- 32 Yan, W., Topphoff, M., Rose, C., and Gmehling, J.: Prediction of vapor-liquid equilibria in
33 mixed-solvent electrolyte systems using the group contribution concept, *Fluid Phase*
34 *Equilibr.*, 162, 97-113, 1999.
- 35 Yu, S. C., Dennis, R., Roselle, S., Nenes, A., Walker, J., Eder, B., Schere, K., Swall, J., and
36 Robarge, W.: An assessment of the ability of three-dimensional air quality models with
37 current thermodynamic equilibrium models to predict aerosol NO₃⁻, *J Geophys Res-Atmos*,
38 110, Artn D07s13
39 10.1029/2004jd004718, 2005.
- 40 Zaveri, R. A., Easter, R. C., and Wexler, A. S.: A new method for multicomponent activity
41 coefficients of electrolytes in aqueous atmospheric aerosols, *J Geophys Res-Atmos*, 110,
42 10.1029/2004jd004681, 2005a.

1 Zaveri, R. A., Easter, R. C., and Peters, L. K.: A computationally efficient Multicomponent
2 Equilibrium Solver for Aerosols (MESA), *J. Geophys. Res.-Atmos.*, 110, 2005b.

3 Zaveri, R. A., Easter, R. C., Fast, J. D., and Peters, L. K.: Model for Simulating Aerosol
4 Interactions and Chemistry (MOSAIC), *J. Geophys. Res.-Atmos.*, 113, 2008.

5 Zhang, Y., Seigneur, C., Seinfeld, J. H., Jacobson, M., Clegg, S. L., and Binkowski, F. S.: A
6 comparative review of inorganic aerosol thermodynamic equilibrium modules: similarities,
7 differences, and their likely causes, *Atmos Environ*, 34, 117-137, Doi 10.1016/S1352-
8 2310(99)00236-8, 2000.

9 Zhang, Y., Pun, B., Vijayaraghavan, K., Wu, S. Y., Seigneur, C., Pandis, S. N., Jacobson, M.
10 Z., Nenes, A., and Seinfeld, J. H.: Development and application of the model of aerosol
11 dynamics, reaction, ionization, and dissolution (MADRID), *J Geophys Res-Atmos*, 109, Artn
12 D01202
13 10.1029/2003jd003501, 2004.

14 Zuend, A., Marcolli, C., Luo, B. P., and Peter, T.: A thermodynamic model of mixed organic-
15 inorganic aerosols to predict activity coefficients, *Atmos. Chem. Phys.*, 8, 2008.

16 Zuend, A., Marcolli, C., Booth, A. M., Lienhard, D. M., Soonsin, V., Krieger, U. K., Topping,
17 D. O., McFiggans, G., Peter, T., and Seinfeld, J. H.: New and extended parameterization of
18 the thermodynamic model AIOMFAC: calculation of activity coefficients for organic-
19 inorganic mixtures containing carboxyl, hydroxyl, carbonyl, ether, ester, alkenyl, alkyl, and
20 aromatic functional groups, *Atmos. Chem. Phys.*, 11, 9155-9206, 2011.

21
22

1 **Tables:**

2 Table 1. Description of activities implemented in SPACCIM.

| Activities | Description |
|---|---|
| Activity of a gas over a particle surface | $\{A_{(g)}\} = p_{A,s}$ |
| Activity of an un-dissociated compound | $\{A_{(aq)}\} = m_A \gamma_A$ |
| Activity of an ion in solution | $\{A^+\} = m_{A^+} \gamma_{A^+}$ |
| Activity of liquid water in a particle | $\{H_2O_{(aq)}\} = a_w$ |
| Activity of a solid | $\{A_{(s)}\} = m_s$, i. e., $\gamma_s = 1$ |

3

4

1 **Figures:**

2

3 Fig. 1: Schematic of the model coupling strategy and its implementation considering the
4 treatment of solution non-ideality and surface tension effects in SPACCIM.

5

6 Fig. 2: Scheme of activity coefficients and surface tension used in the microphysics and
7 multiphase chemistry models.

8

9 Fig. 3: Sparse structure of Jacobian and two droplet classes [adapted from Wolke et al.
10 (2005)].

11

12 Fig. 4: Scheme of the currently used interactions in the MR and SR part. Parameters for ion
13 \leftrightarrow ion and ion \leftrightarrow organic main group interactions are all incorporated in the MR part and set
14 to zero in the SR (UNIFAC) part.

15

16 Fig. 5: Comparison with measurements of aqueous electrolyte solutions (symbols) and
17 corresponding calculations of the models E-AIM/AIM III (Clegg et al., 1998b), mod. LIFAC
18 (Kiepe et al., 2006), Ming and Russell (Ming and Russell, 2002) and SpactMod at 298 K for
19 the salt NaCl + NH₄NO₃ at a molar salt mixing ratio of (3:1). Note that SpactMod reproduces
20 the results of AIOMFAC (Zuend et al., 2008) due to the same parameters applied.

21

22 Fig. 6: Intercomparison between selected models for Ca(NO₃)₂ salt: : Water activities (solid
23 lines) and mean activity coefficients (dashed lines). Again, SpactMod reproduces AIOMFAC.

24

25 Fig. 7: Comparison between experimental and calculated water activities (a_w) in aqueous
26 citric acid solutions as a function of water fraction (x_w) at 298.15K. Experimental data are
27 taken from Maffia and Meirelles (2001).

28

29 Fig. 8: Comparison between experimental (symbols) and calculated mean activity coefficients
30 (solid lines) of binary salt mixtures as a function of molality (mol kg⁻¹) at 298 K.
31 Experimental data are taken from Hamer and Wu (1972).

32

33 Fig. 9: Comparison of modeled water activities for the aqueous solution composed of organic-
34 electrolyte mixture: (NH₄)₂SO₄ + Glycerol + H₂O [(2:1:1) mole ratio]. The SpactMod results
35 are in agreement with AIOMFAC.

36

37 Fig. 10: Comparison between measured and modeled water activities for the aqueous solution
38 composed of organic-electrolyte mixture: (NH₄)₂SO₄ + Ethanol + Acetic acid [(2:1:1) mole
39 ratio].

40

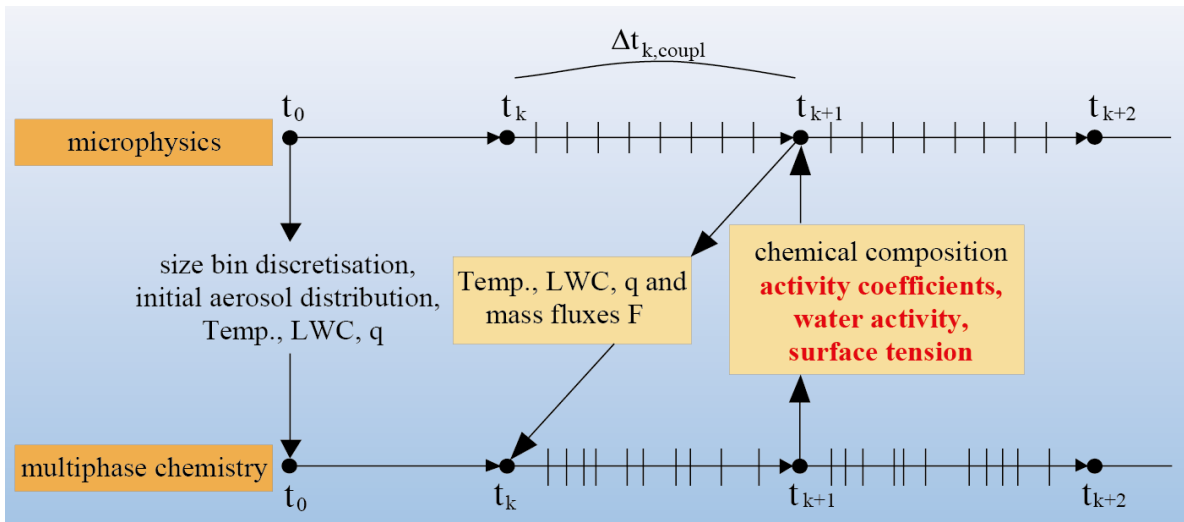
41 Fig. 11: Importance of different interactions in the aqueous solution composed of NaCl +
42 (NH₄)₂SO₄ + Ethanol + Malonic acid [1:1:1:1 (mole ratio)].

43

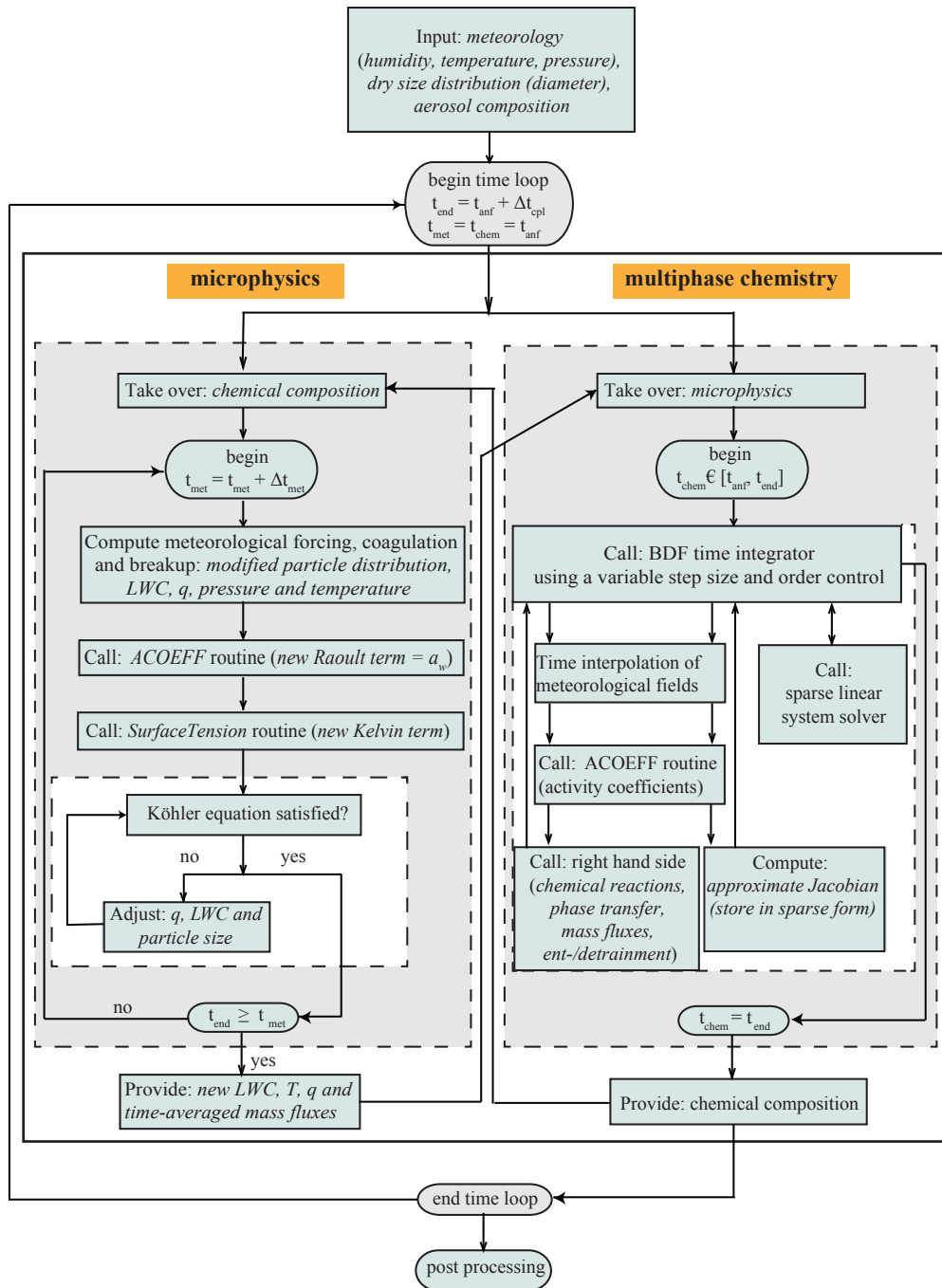
44 Fig. 12: Modeled activity coefficients of main inorganic particle phase constituents (top) and
45 important transition metal ions (TMIs, down) as the function of the simulation time for the
46 two different relative humidity cases (left: 90% r.h., right: 70% r.h.). The blue bars mark the
47 in-cloud time periods during the simulation time.

48

1 Fig. 13: Modeled activity coefficients of organic carbonyl compounds (top) and organic
2 acids/anions (TMIs, down) as the function of the simulation time for the two different relative
3 humidity cases (left: 90% r.h., right: 70% r.h.). The blue bars mark the in-cloud time periods
4 during the simulation time.
5
6 Fig. 14: Modeled pH values as the function of the simulation time for the two different
7 relative humidity cases (left: 90% r.h., right: 70% r.h.) considering ideal (red line) and
8 non-ideal (blue line) solutions, respectively. The blue bars mark the in-cloud time periods
9 during the simulation time.
10



1
2 Fig. 1
3



1
2 Fig. 2

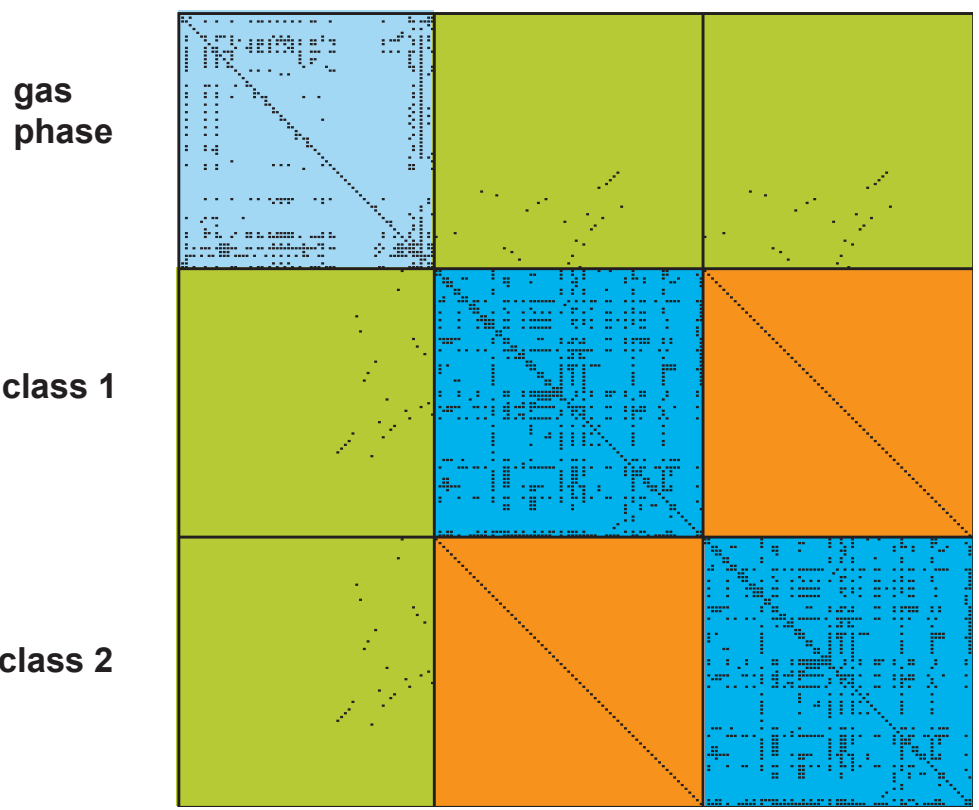


Fig. 3

1
2
3

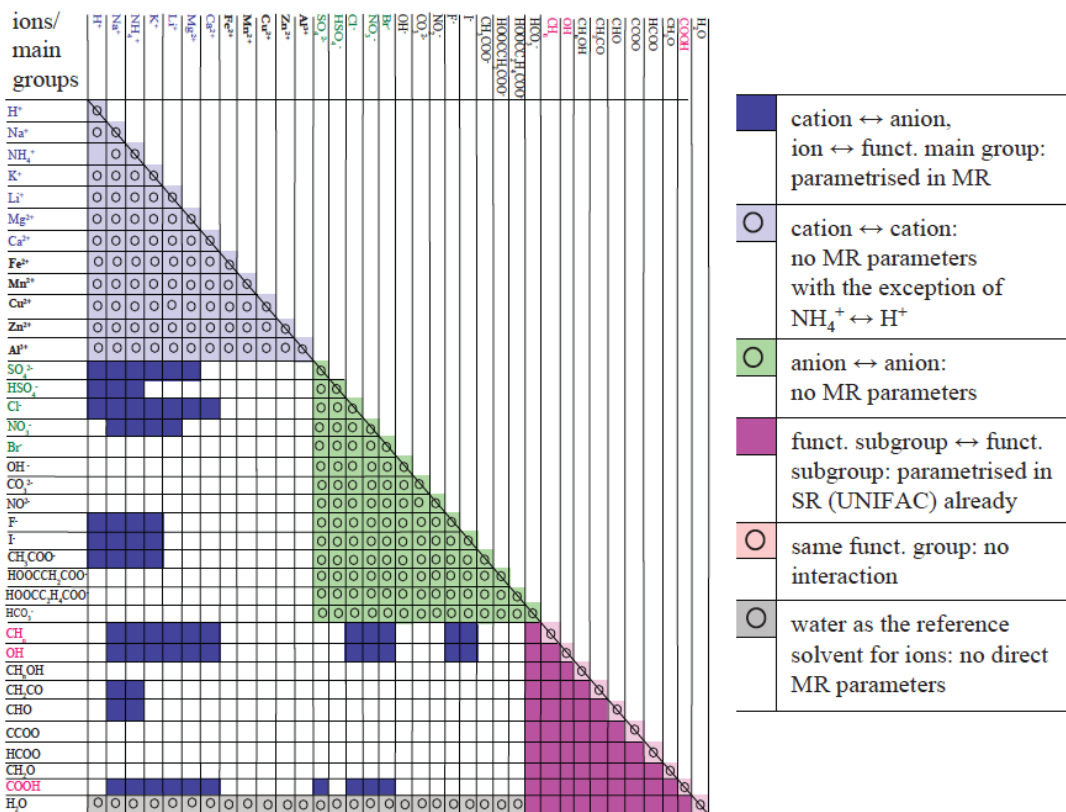
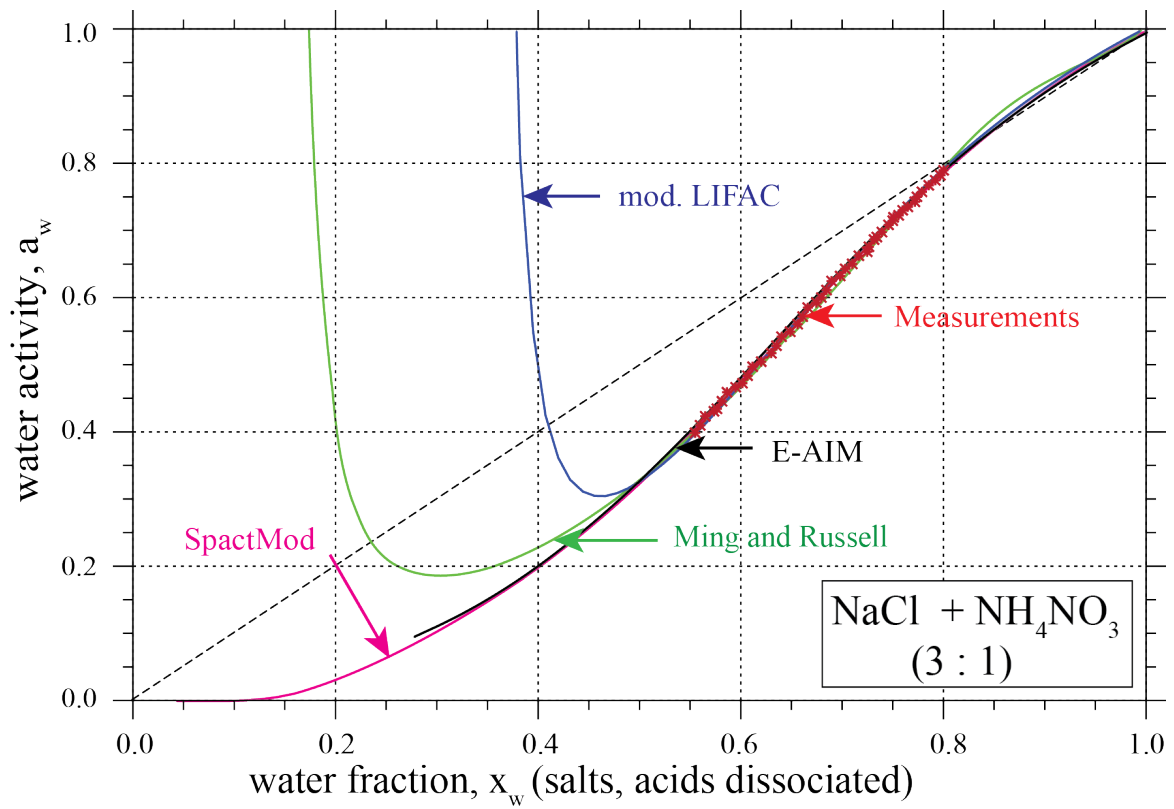


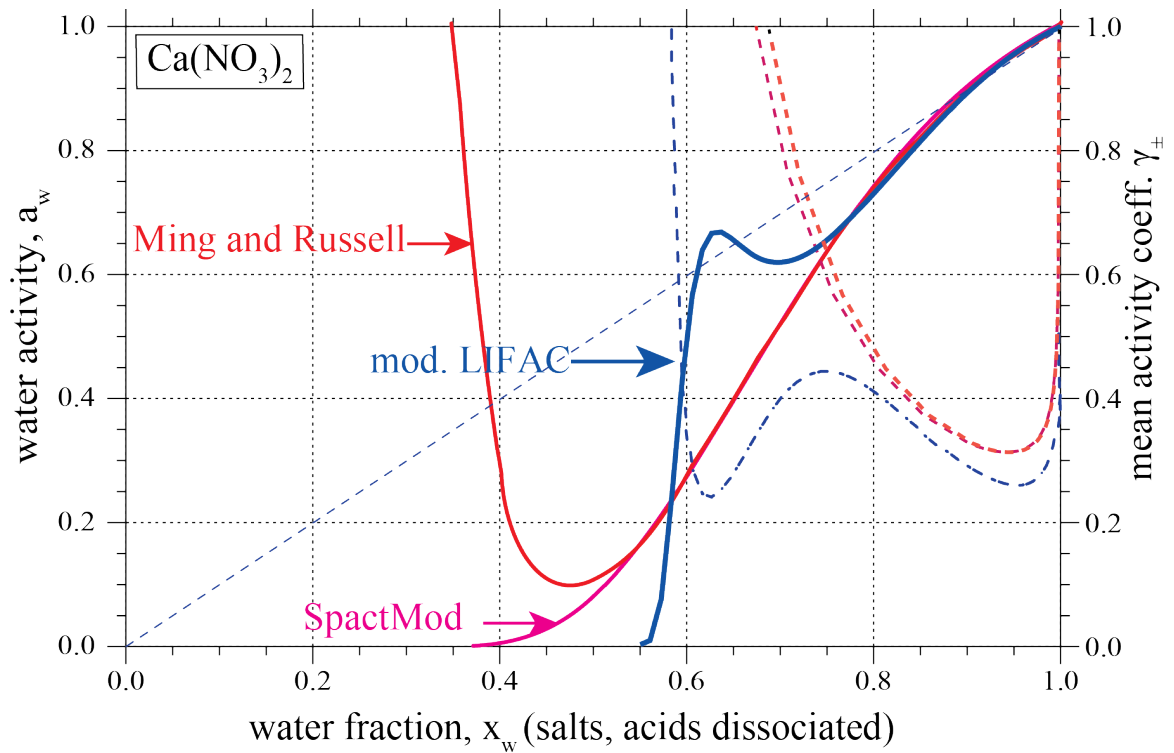
Fig. 4

4
5
6



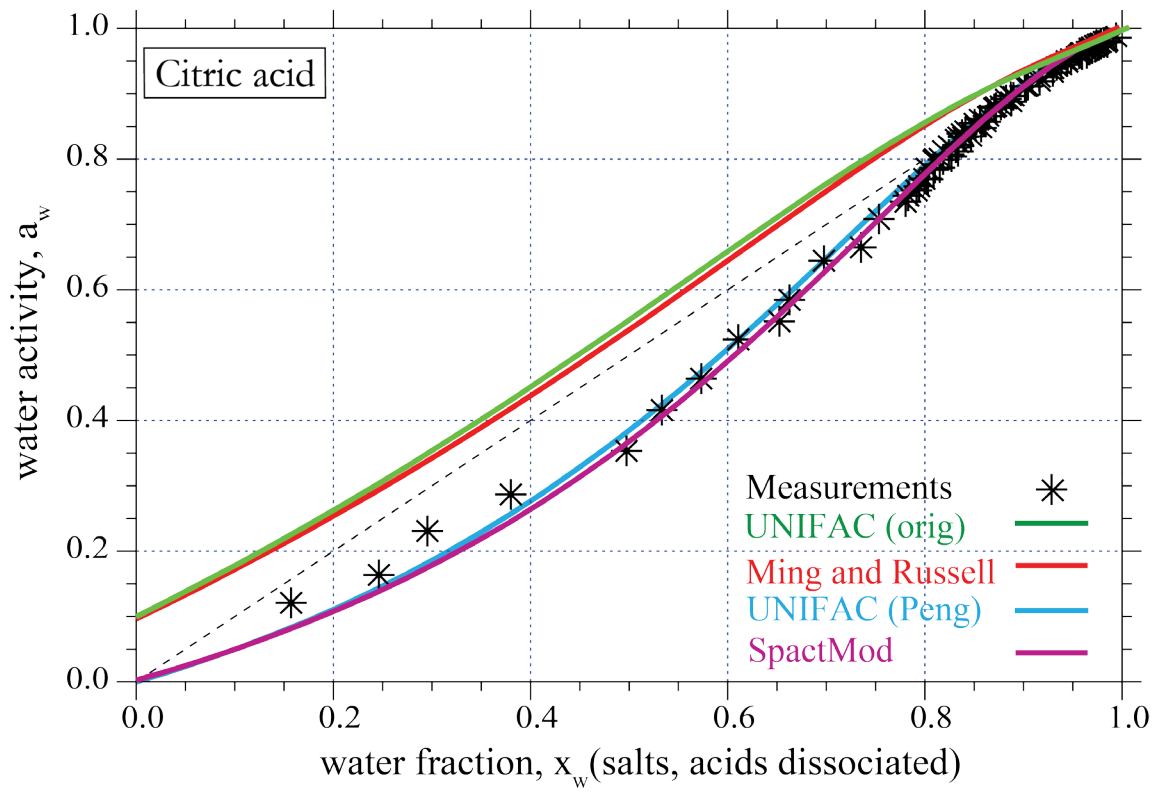
1
2
3

Fig. 5

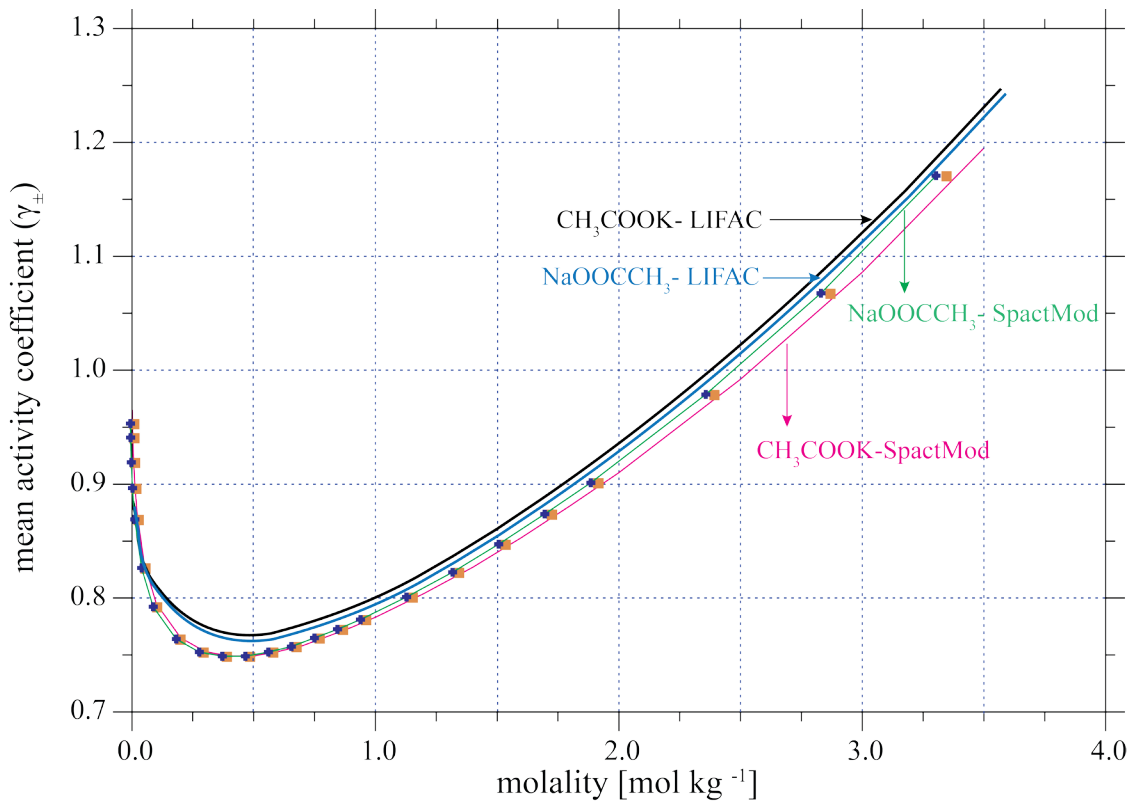


4
5
6

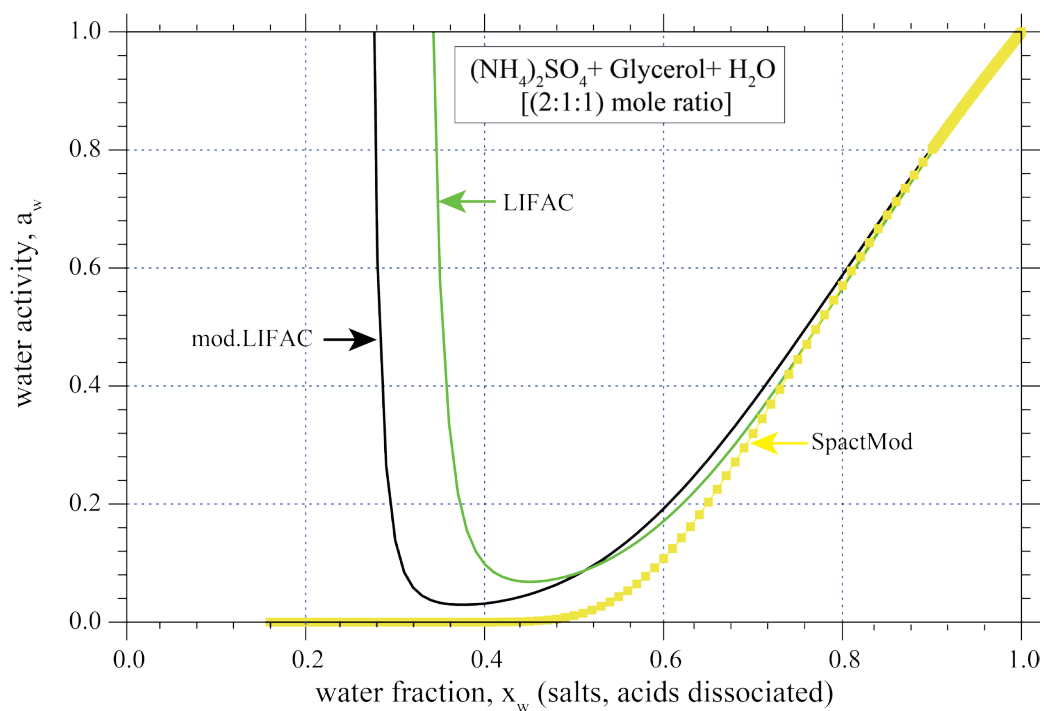
Fig. 6:



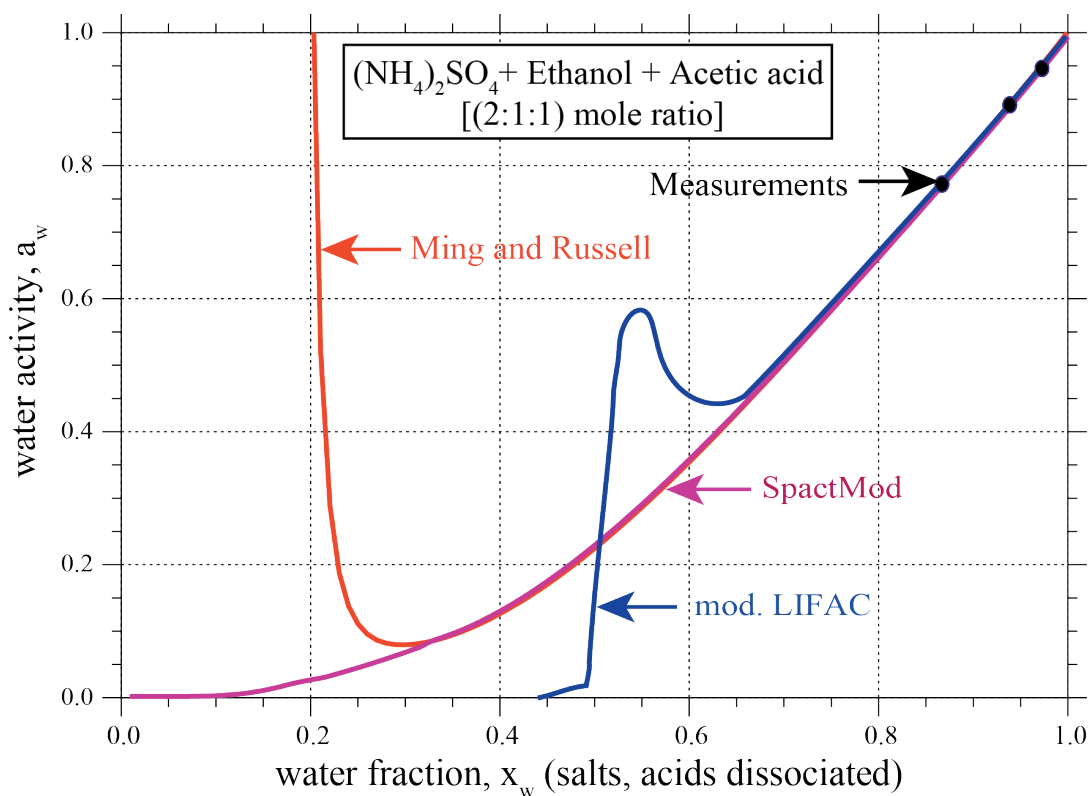
1
2
3
4
Fig. 7



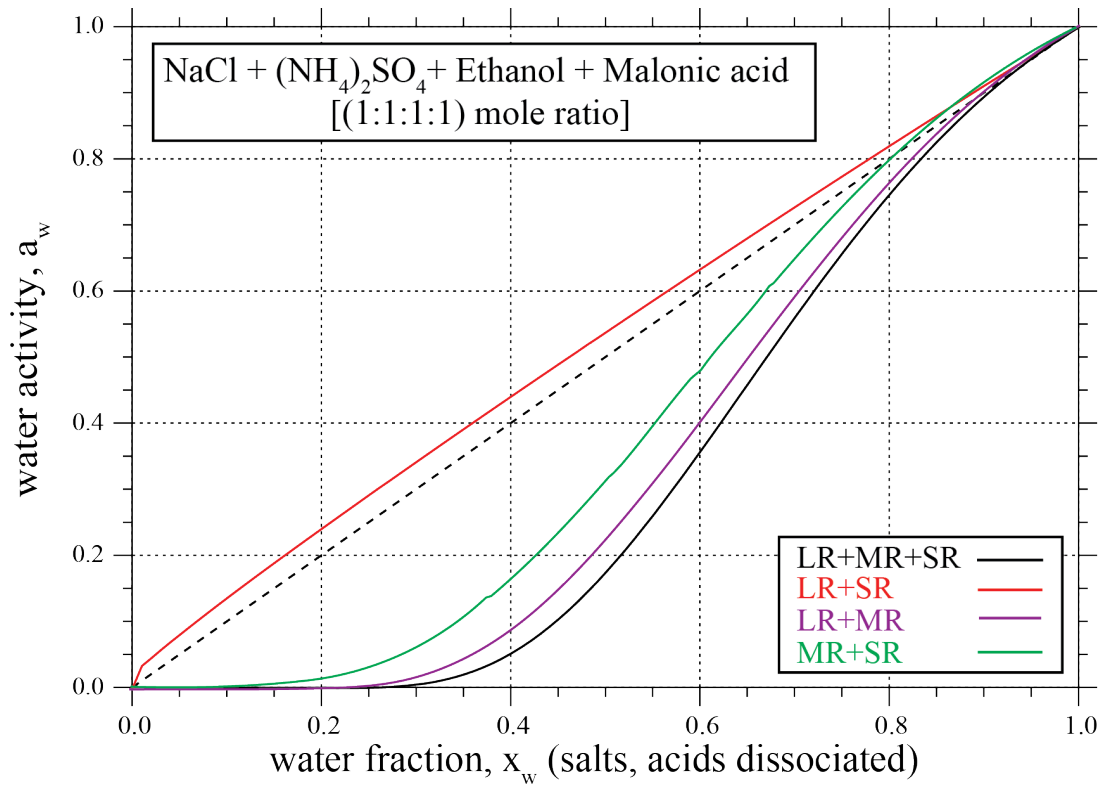
5
6
7
8
Fig. 8



1
2 Fig. 9
3
4
5

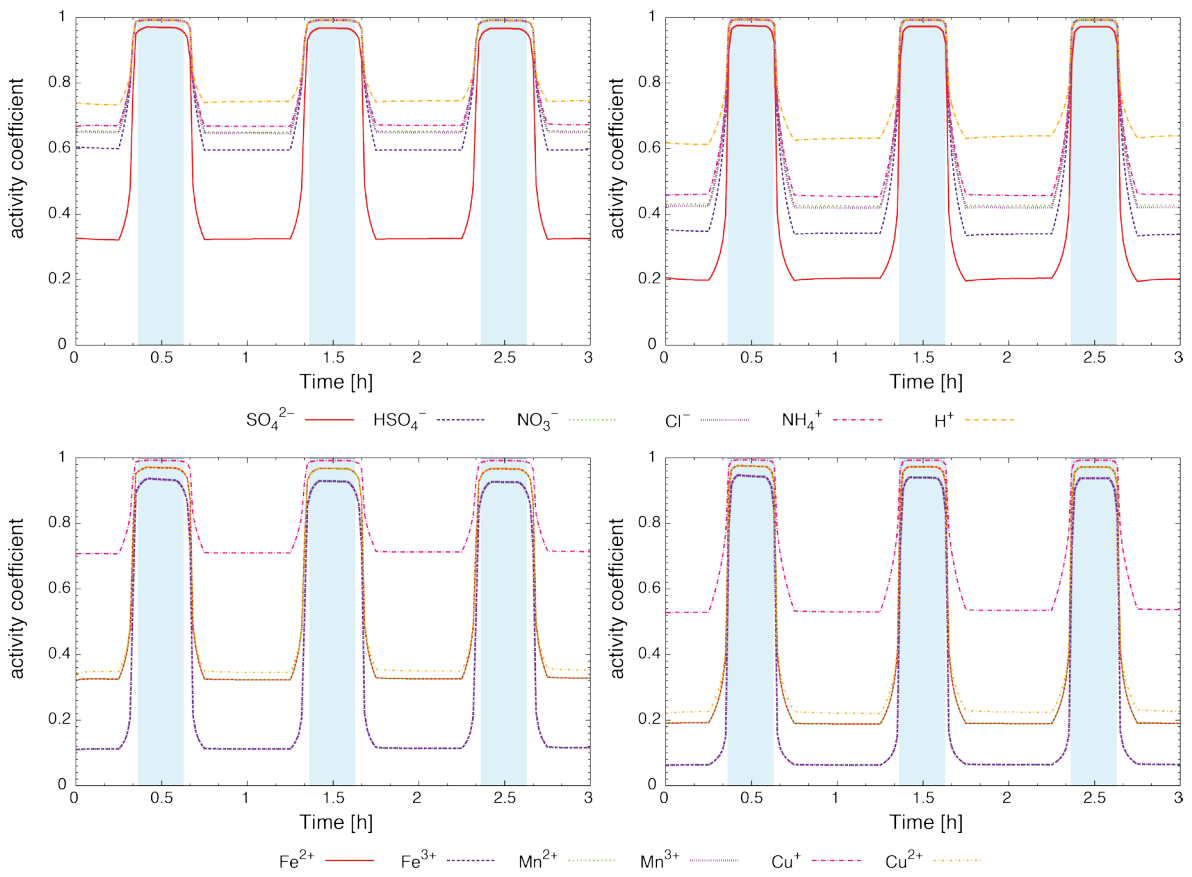


6
7 Fig. 10
8



1
2
3
4

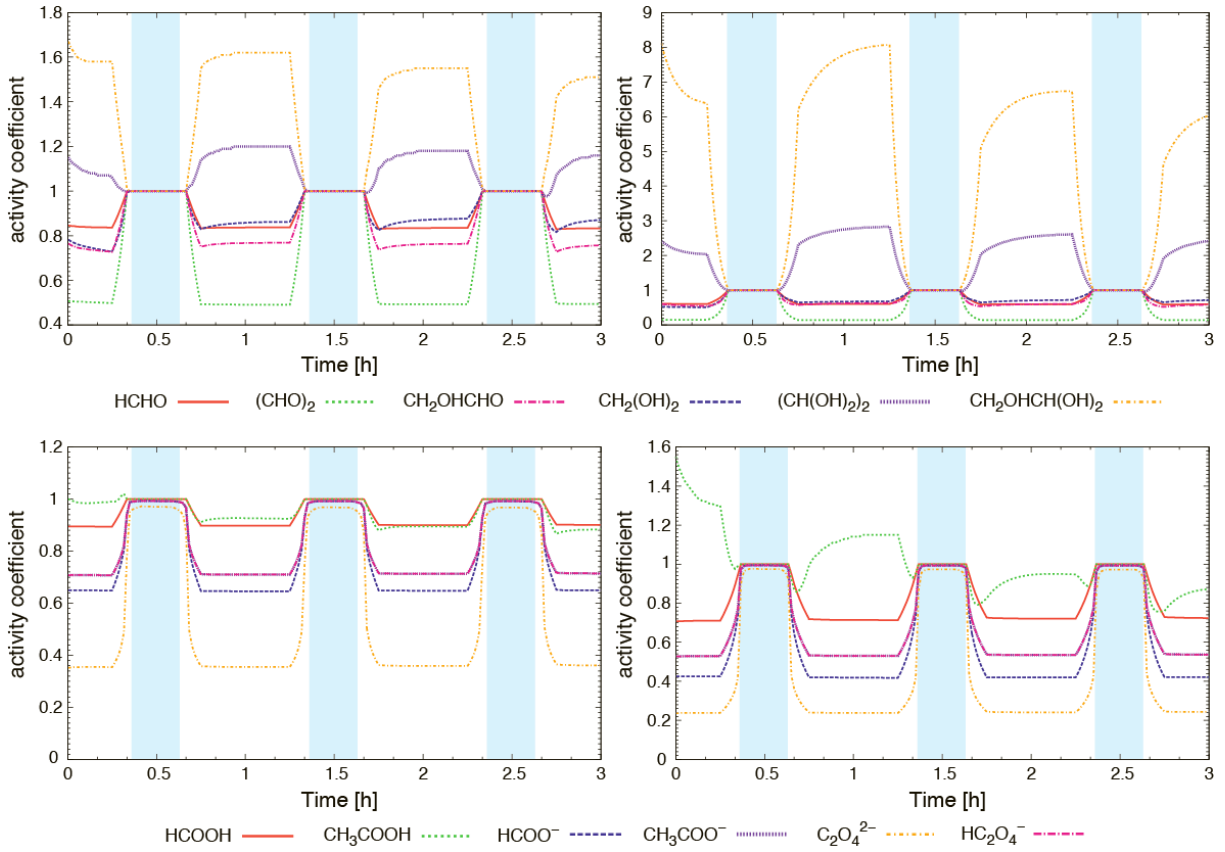
Fig. 11



5
6

Fig. 12

1



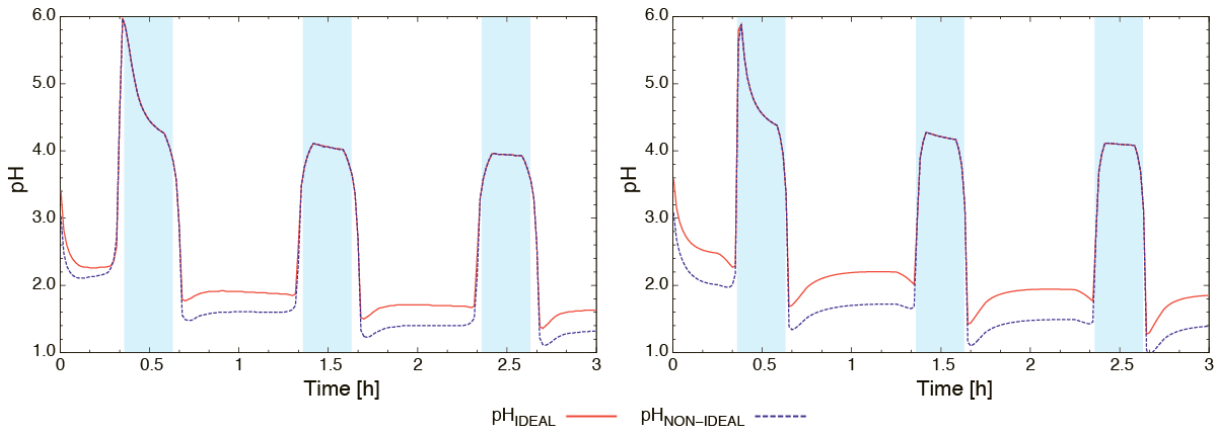
2

3

Fig. 13

4

5



6

7

Fig. 14

8